

1 METHANE AS A DIAGNOSTIC TRACER OF CHANGES IN THE BREWER-DOBSON
2 CIRCULATION OF THE STRATOSPHERE

3 Ellis E. Remsberg

4 Science Directorate

5 NASA Langley Research Center

6 21 Langley Blvd., Mail Stop 401B

7 Hampton, VA 23681, USA

8 Ellis.E.Remsberg@nasa.gov

9
10 **Abstract.** This study makes use of time series of methane (CH₄) data from the Halogen
11 Occultation Experiment (HALOE) to detect whether there were any statistically significant
12 changes of the Brewer-Dobson Circulation (BDC) within the stratosphere during 1992-2005.
13 The HALOE CH₄ profiles are in terms of mixing ratio versus pressure-altitude and are binned
14 into latitude zones within the southern and the northern hemisphere. Their separate time series
15 are then analyzed using multiple linear regression (MLR) techniques. The CH₄ trend terms for
16 the northern hemisphere are significant and positive at 10°N from 50 hPa to 7 hPa and larger
17 than the tropospheric CH₄ trends of about 3 %/decade from 20 hPa to 7 hPa. At 60°N the trends
18 are clearly negative from 20 hPa to 7 hPa. Their combined trends indicate an acceleration of the
19 BDC in the middle stratosphere of the northern hemisphere during those years, most likely due to
20 changes from the effects of wave activity. No similar significant BDC acceleration is found for
21 the southern hemisphere. Trends from HALOE H₂O are analyzed for consistency. Their mutual
22 trends with CH₄ are anti-correlated qualitatively in the middle and upper stratosphere, where CH₄
23 is chemically oxidized to H₂O. Conversely, their mutual trends in the lower stratosphere are
24 dominated by their trends upon entry to the tropical stratosphere. Time series residuals for CH₄
25 in the lower mesosphere also exhibit structures that are anti-correlated in some instances with
26 those of the tracer-like species HCl. Their occasional aperiodic structures indicate the effects of
27 transport following episodic, wintertime wave activity. It is concluded that observed multi-year,
28 zonally-averaged distributions of CH₄ can be used to diagnose major instances of wave-induced
29 transport in the middle atmosphere and to detect changes in the stratospheric BDC.

1
2
3
4
5
6
7
8
9
10
11
12
13
14
15
16
17
18
19
20
21
22
23
24
25
26
27

1 Background

The dynamically-forced, seasonal circulation in the meridional plane of the stratosphere is balanced by differential radiative heating between Equator and Pole. It is a measure of the diabatic circulation and is often termed the residual mean mass circulation or the Transformed Eulerian Mean (TEM) circulation (e.g., Dunkerton, 1978; Andrews et al., 1987). To a large degree, that primary circulation is balanced at the middle latitudes by two-way exchanges or mixing processes (Birner and Bönisch, 2011; Garny et al., 2014; Ploeger et al., 2015a). Together, both mechanisms constitute the total or Brewer-Dobson circulation (BDC), generally having an upward component at low latitudes and a return, downward component at the extratropical latitudes of both the northern and the southern hemispheres (e.g., Butchart, 2014; Plumb, 2007; Haynes et al., 1991). The dissipation of planetary (or Rossby) waves and gravity wave forcings tends to accelerate the BDC and to enhance mixing in the winter hemisphere (e.g., Solomon et al., 1986; Plumb, 2007; Shepherd, 2007; Okamoto et al., 2011). Thus, it is likely that there is some asymmetry for the BDC in the northern versus the southern hemisphere stratosphere because winter wave forcing and mixing processes are more pronounced and frequent in the northern hemisphere (Shepherd, 2007).

A schematic of the BDC and its relation to the distribution of ozone in the stratosphere is shown in Fig. 1 for March, where the solid black curves represent the sense of the circulation and the vertical orange arrow represents the approximate region for the propagation of waves from the upper troposphere and up into the middle atmosphere (see Shaw and Shepherd, 2008). Figure 1 indicates that the BDC leads to an accumulation of ozone in the extratropics of the northern hemisphere by March. Tracer-like molecules, such N₂O and CH₄, exhibit distributions that are well correlated and vary seasonally in response to changes in the BDC (Plumb and Ko, 1992; Holton, 1986).

1 Figure 2 is an example of the zonally-averaged distribution of CH₄ for January from a
2 NASA/Goddard, two-dimensional chemistry and transport model simulation (Fleming et al.,
3 1999). The white arrows show the effects of the stratospheric BDC, which is strong in the winter
4 hemisphere (longer arrows) and weak in the summer stratosphere. Tracer species such as CH₄
5 depict the mass circulation qualitatively, i.e., bulging upward in the tropics and downward at
6 high latitudes (more so in the winter hemisphere). Figure 2 shows that the January zonal-mean
7 circulation is in the correct sense to bring about the accumulation of ozone in the lower
8 stratosphere by March, as shown in Fig. 1. In addition, Manney et al. (1994) emphasize that the
9 character of the observed winter hemisphere transport and descent differs for the upper versus
10 the lower stratosphere and depends on whether the polar vortex is undisturbed and centered on
11 the Pole or disturbed by Rossby-wave activity.

12

13 A current issue is whether the observed, seasonal BDC is changing in the presence of the steady
14 increases in the so-called “greenhouse gases”, like CO₂ (e.g., Butchart, 2014). Early on, Rind et
15 al. (1990) conducted a series of simulation studies of those effects, and their results indicated that
16 there will be an acceleration of the BDC, particularly in the northern hemisphere. Lin and Fu
17 (2013) analyzed more recent results from a collection of chemistry/climate models (CCM), and
18 they found that the diabatic effects from changes in the ozone and CO₂ are likely driving
19 observed changes in the meridional temperature gradients and of the BDC of the lower
20 stratosphere. Based on the results of the CCM studies, they decomposed the BDC into a
21 transition (100-70 hPa) branch, a shallow (70-30 hPa) branch, and a deep (30 hPa and higher)
22 branch. Further, the CCM studies predict an acceleration of the BDC that will affect the rate of
23 recovery for the ozone layer in the lower stratosphere.

24

25 Observational evidence for the diagnosis of a long-term acceleration of the several branches of
26 the BDC and their associated mean age-of-air (AoA) is somewhat ambiguous from time series of
27 stratospheric temperatures (Butchart, 2014). However, recently Diallo et al. (2012, Fig. 13) and
28 Monge-Sanz et al. (2012, Fig. 3) found a decrease of mean AoA in the shallow branch and an

1 increase of AoA in the deep branch of the BDC for the ERA-Interim time period of about 1989-
 2 2010. Alternatively, Garcia et al. (2011) recommended obtaining AoA using observed chemical
 3 tracers that are well sampled, have linear (CO₂) or exponential (SF₆) growth rates, and no
 4 chemical loss in the stratosphere. To that end, Ray et al. (2014), Stiller et al. (2012), and Ploeger
 5 et al. (2015a) have successfully employed measured profiles of CO₂ and SF₆ to diagnose trends
 6 in the AoA or the BDC and to separate the effects of the residual circulation from the effects of
 7 mixing processes. Their analyses apply to pressure altitudes or potential temperatures of the
 8 lower stratosphere (16 to 30 km). What about other chemical tracers? For example, hydrogen
 9 fluoride (HF) is a stratospheric end product of the photochemical conversion from
 10 chlorofluorocarbon (CFC) molecules but has been increasing non-linearly, so it is not a good
 11 candidate for such studies. H₂O has shown long-term increases of about 0.6%/yr (Scherer et al.,
 12 2008), but H₂O entering the stratosphere from below is subject to seasonal and occasional
 13 episodic changes of the temperature at the tropical tropopause. On the other hand, CH₄ exhibits a
 14 small, monotonic, and nearly linear, annually-averaged trend in the troposphere (see Sect. 5 for
 15 more details), and CH₄ is unaffected during its upward transport through the tropical tropopause.

16

17 Generally, it is not possible to diagnose AoA or an acceleration of the BDC solely from a time
 18 series of a chemical tracer like CH₄ because its mixing ratio, $\chi(r,t)$, at a specific location r in the
 19 stratosphere is the integral of the product in expression (1) below for all past times t' from $-\infty$ to
 20 t , where $\chi_0(t')$ is the time series for CH₄ in the troposphere, $G(r,t')$ is the stratospheric age spectra
 21 or transit time distribution (its first momentum being the mean AoA), and $L(r,t')$ is its loss
 22 function that depends on the path spectra and the chemical sink distribution for CH₄ in the
 23 stratosphere (Volk et al., 1997).

$$24 \quad \chi_0(t') G(r,t') L(r,t') \quad (1)$$

25 The source function, $\chi_0(t')$, is estimated to have a trend of about 3 %/decade from 1990 to 2003,
 26 as discussed later in Sect. 5. The loss function at a given stratospheric location, $L(r,t')$, is related
 27 to the decay of the tracer along the complete path spectrum (all pathways from the entrance
 28 region, or tropical tropopause, to the specific location), and only tracers with constant

1 tropospheric values and of a radioactive decaying type within the stratosphere are truly path
2 independent (Hall and Plumb, 1994). Even if the time series for the CH₄ source gas is
3 approximately linear, it should be clear from Fig. 2 that $L(r,t')$ is spatially inhomogeneous in
4 both the vertical and meridional directions. One cannot easily sort out the components of
5 changes in the mean AoA from changes in the path spectra (Schoeberl et al., 2000). However, to
6 first approximation, both the path and loss function L can be assumed stationary, such that CH₄
7 in the stratosphere is a fraction (f) of the tropospheric CH₄ and where f is a function of
8 latitude/height and season (e.g., Fueglistaler, 2012). Deviations from this scenario are
9 interpreted in the present study as being indicative of changes in the age spectra G , rather than L .
10 This approximation follows from the idea that the chemical effects of changes in stratospheric
11 composition for the methane oxidation rates are small. The tropospheric trends for the CH₄
12 source gas are small, and the annually-averaged, chemical loss term for CH₄ in the stratosphere
13 should give rise to spatial gradients that are very nearly symmetric across the two hemispheres.
14 Despite those considerations for hemispheric symmetry, the analyses of time series of observed
15 stratospheric CH₄ show that their long-term trends differ between the northern and southern
16 hemispheres and indicate significant changes from the effects of mixing on the BDC in the
17 middle stratosphere of each hemisphere.

18

19 **2 Objectives**

20 The modeled CH₄ distribution in Fig. 2 is very similar to observed wintertime distributions of
21 CH₄ from satellite datasets. CH₄ is decreasing with pressure-altitude and with latitude because
22 CH₄ is oxidized in a multi-step process to H₂O in the middle and upper stratosphere (e.g.,
23 Brasseur and Solomon, 2005). In an early study using CH₄ data from the Stratospheric and
24 Mesospheric Sounder (SAMS) on Nimbus 7, Stanford and Ziemke (1991) determined
25 empirically that the minimum lifetime for its chemical conversion to H₂O is of the order of 3 to 4
26 months at low latitudes in the upper stratosphere or somewhat longer than the time constants for
27 the mean meridional transport. Holton and Choi (1988) and Stanford et al. (1993) used the three
28 years of SAMS CH₄ data as a tracer for the characterization of the vertical and meridional
29 components of the seasonal net transport. The present analysis study makes use of time series of

1 CH₄ mixing ratio data as a function of pressure-altitude for 1992-2005 from the Halogen
2 Occultation Experiment (HALOE) aboard the Upper Atmosphere Research Satellite (UARS).
3 As noted by Rosenlof (2002) and by Neu et al. (2003), atmospheric sampling via the method of
4 solar occultation is adequate typically for obtaining the large-scale seasonal variations of CH₄.

5

6 The HALOE instrument obtained sunrise (SR) and sunset (SS) profiles of CH₄ in the stratosphere
7 and lower mesosphere, and a number of researchers have made use of its CH₄ data for studies of
8 middle atmosphere transport. Ruth et al. (1997), Randel et al. (1998), Gray and Russell (1999),
9 Randel et al. (1999), and later Shu et al. (2013) used the multi-year distributions of the HALOE
10 CH₄ mixing ratio as a tracer for the effects of the semi-annual oscillation (SAO) and quasi-
11 biennial oscillation (QBO) forcings. Youn et al. (2006) analyzed time series of CH₄, H₂O, and
12 HF from HALOE for their trends at 10 hPa and in one latitude zone, 40 to 45 degrees, and they
13 found differences in their trends between the two hemispheres. They related the trends that they
14 found for the northern hemisphere to an intensification of stratospheric wave activity over that
15 14-yr time span.

16

17 The present study is an analysis of time series of the HALOE CH₄ for an increasing (positive)
18 trend in the tropical ascent and for a correspondingly increasing (negative) trend in the
19 extratropical descent in the same hemisphere. Multiple linear regression (MLR) techniques are
20 used for the analyses and are discussed in Section 3, and they fit the seasonal and the
21 interannually-varying forcings along with the trend terms in time series of CH₄ as a function of
22 latitude and pressure-altitude. Preliminary MLR model results are also shown in Sect. 3, and
23 concerns about having an adequate number of profile samples for each of the SR and SS
24 crossings of a latitude zone are addressed in Section 4. Final sets of CH₄ time series are selected
25 as representative of the tropical and extratropical latitude zones of each hemisphere, as depicted
26 in the simple schematic of Plumb (2007, his Fig. 13). An estimate of the trends for the CH₄
27 source gas is presented in Section 5. Then the coefficients of the stratospheric trend terms from
28 HALOE and their statistical significance are given and compared with that of the source gas for

1 each latitude zone and as a function of pressure-altitude. Trends from the study herein are
2 compared with those reported by other groups, which in some instances were based only on
3 HALOE data through the 1990s.

4

5 Trends from analyses of HALOE H₂O are shown in Section 6 and compared with those of CH₄
6 for consistency, since H₂O is the primary chemical product of CH₄ oxidation at the upper
7 altitudes. Section 6 also relates the time series of residuals from analyses of CH₄ in the lower
8 mesosphere to de-seasonalized variations in HCl, another molecule that contains information
9 about the BDC of the stratosphere and mesosphere. In particular, it is shown that the residuals
10 from the separate MLR fits to the CH₄ and HCl series have small, irregular variations of opposite
11 sign. It is posited that the somewhat anomalous variations in the multi-year time series of
12 HALOE HCl for the lower mesosphere that have been reported by others are due to effects from
13 anomalous wave forcings during 1999-2002. Section 7 is a summary of findings from the
14 present analyses.

15

16 **3 Analysis approach**

17 Effects from the seasonal BDC are apparent from monthly, zonal-mean cross sections of CH₄, as
18 shown by Holton and Choi (1988) from the SAMS data and by Randel et al. (1998) and Shu et
19 al. (2013) from the HALOE data. Qualitatively, there is a net upward transport of CH₄ at the low
20 latitudes, a net poleward transport throughout the stratosphere, plus a descent of CH₄-poor air
21 within the polar vortex beginning at upper altitudes (cf., Fig. 2). The monthly CH₄ distributions
22 also exhibit a significant, negative mixing ratio gradient from the tropics to higher latitudes along
23 pressure surfaces in the middle and upper stratosphere. The exact latitude location of the
24 maximum gradient varies seasonally, according to the strength of the meridional mixing of the
25 air masses that occurred in the weeks before. Latitude versus pressure-altitude cross sections of
26 the CH₄ from the HALOE Website (<http://haloe.gats-inc.com/home/>) for October of successive
27 years reveal that the isolines of the tropical CH₄ distribution did not extend into the upper
28 stratosphere during 1991, 1993, 1995, 1997, 1999, and 2004, while they were elevated in 1992,

1 1994, 1998, 2002, and 2003. CH₄ variations for 1996, 2000, and 2001 were intermediate to
2 those of the other years. Gray and Russell (1999) and Shu et al. (2013) showed that the apparent,
3 interannual strength or upward extent of the CH₄ due to the mean meridional circulation is
4 related to the phase of the QBO and/or to the effects of the Rossby-wave forcing. To first order,
5 the isolines of the CH₄ in Fig. 2 and in the HALOE data also indicate that there are distinct BDC
6 branches in the northern hemisphere and in the southern hemisphere.

7

8 Points for the data time series of the present study are generated using the HALOE version 19,
9 Level 2 CH₄ profiles from occurrences of the HALOE SR or SS observations within a latitude
10 zone for 1992-2005, as in Remsberg (2008). The SR and SS profiles are binned into 14
11 overlapping latitude zones from 65°S to 65°N and at 12 pressure-altitudes, giving a total of 168
12 separate time series for analysis. Initially, the width of each latitude bin was set to 20 degrees,
13 ensuring a relatively large number of samples. Example time series for the southern and
14 northern extratropics are shown in Fig. 3 at 10 hPa (near 31 km). Each data point in Fig. 3 is an
15 approximate snapshot of the zonally-averaged CH₄ for the latitude zone (cf., Fig. 2). The
16 oscillating curves in Fig. 3 are the MLR fits to the data points from mid-1992 onward and based
17 on the terms indicated at the lower left of the figure. The near horizontal line is the sum of the
18 constant and linear trend terms of the MLR model.

19

20 Results of similar MLR analyses of time series of HALOE data were reported for ozone
21 (Remsberg, 2008), temperature (Remsberg, 2009), and mesospheric water vapor (Remsberg,
22 2010). Details of the formulation of the terms for the MLR models can be found in Remsberg
23 (2008) and are summarized here. Initially, only semiannual (SAO) and annual (AO) terms are
24 considered for the model. A Fourier analysis is then applied to the residual or difference of the
25 model values from the points in the time series, in order to identify significant periodic,
26 interannual terms that remain. Three interannual terms are almost always present and are
27 included in the model: an 838-dy (27.5-mo) or QBO1 term; a small amplitude, 718-dy (23.5-
28 mo) biennial or QBO2 term; and a 690-dy (22.6-mo) sub-biennial (SB) term, whose period arises

1 from the difference interaction between QBO and annual terms. The relative amplitudes of these
2 three interannual terms vary with latitude and altitude (see also Baldwin and Dunkerton, 1998).
3 The 22.6-mo term agrees closely with the anti-symmetric empirical orthogonal function (EOF)
4 identified by Dunkerton (2001, his Eq. (5.2)) for the subtropical latitudes from a shorter series of
5 HALOE CH₄ data. The primary purpose of identifying and including interannual terms in the
6 MLR model is so that their significant structures can be accounted for. A linear trend term is
7 also part of the final models. Lag-1 autocorrelation (AR-1) effects are a significant part of the
8 MLR models for zonally-averaged stratospheric data. The accounting for AR-1 effects corrects
9 for minor, but important biases between the MLR model and the CH₄ points that often occur
10 along short segments of the data series. Corrections for AR-1 effects follow the two-step
11 approach of Tiao et al. (1990, their Appendix A), and those corrections have a significant impact
12 on the analyzed trend terms.

13

14 Data in the first year following the Mt. Pinatubo eruption of June 1991 often appear to have been
15 perturbed, so that time span is not considered for the MLR fittings. In Fig. 3 (bottom) one can
16 see that there is also a weak, decadal-scale variation in the data series, whose amplitude is
17 characterized by a difference interaction between the QBO1 and SB terms (or near to the 10.6-yr
18 period found by Baldwin and Dunkerton (1998)). However, a separate term with that period is
19 not part of the MLR models of the present study. In addition, Nedoluha et al. (1998) reported
20 that solar cycle (SC) effects on CH₄ are very small even near the stratopause; thus, no 11-yr or
21 SC-proxy term is included in the MLR models. However, there is a cooling of the middle
22 atmosphere during this 14-yr time span, due to the increasing atmospheric CO₂. Therefore, the
23 analyses are conducted for time series of the CH₄ mixing ratio at pressure-altitudes rather than
24 geometric altitudes. In this way, the added effects from the contraction of a pressure surface
25 with altitude and time are avoided. It is further assumed that the age spectrum G is invariant in
26 pressure space if the dynamical forcing is invariant in pressure space. To first order then, the
27 variations of CH₄ with time at a pressure level represent the effects of the diabatic transport
28 vertically within a zone and any horizontal mixing to/from adjacent latitude regions.

29

1 Figure 3 depicts the CH₄ time series for 10 hPa and at 55° latitude for the two hemispheres.
2 Figure 4 shows the associated, annual mean distribution of CH₄ that is based on the constant
3 terms from the MLR models, and the mean mixing ratios for 10 hPa are nearly the same or 0.77
4 ppmv at 55°N and 0.82 ppmv at 55°S. The amplitudes of the SAO and the AO terms in Fig. 3
5 are more distinct in the southern than in the northern hemisphere, despite the fact that the
6 seasonal cycle for the mean meridional circulation of each hemisphere is mainly just a
7 consequence of similar variations in the dynamical forcing between Equator and Pole. Figure 3
8 (bottom) shows that the seasonal maximum occurs in late autumn to early winter in the northern
9 extratropics, and its minimum is in late summer. It may be that the SAO and AO cycles at 55°N
10 are influenced and the annual mean mixing ratio reduced slightly, due to meridional mixing of
11 the air during late winter to spring. On the other hand, Fig. 3 (top) at 55°S shows minimum data
12 values of 0.5 to 0.6 ppmv for some years and most often in late winter, and they are not fit well
13 by the MLR model. That circumstance is because those perturbations in the CH₄ data occur for
14 only a short time (few weeks) in late winter/early spring, or at the time of the final warming in
15 the southern hemisphere; those rapid variations are not resolved by the terms of the MLR model.
16 The amplitudes of the several interannual terms are also significant in the extratropics at 10 hPa.
17 Finally, the trend coefficients from the data of Fig. 3 are slightly positive in the south but
18 negative in the north; that difference is discussed further in Sect. 5.

19
20 Corresponding CH₄ time series at 7 hPa are shown for the two subtropical zones in Fig. 5.
21 Periodic variations in Fig. 5 (top) for the southern hemisphere are primarily from the annual and
22 QBO cycles; its average CH₄ is about 1.1 ppmv. Effects from the SAO term do not emerge
23 clearly until the upper stratosphere (not shown). The data for the northern subtropics in Fig. 5
24 (bottom) indicate a seasonal cycle that is more variable and somewhat weaker than in the south;
25 interannual effects (QBO and SB) are present but are weaker, too. In general, there is less
26 periodic structure in the CH₄ of the northern subtropics at this level, again most likely because of
27 the mixing effects from the dissipation of Rossby waves and gravity waves. Mixing of air from
28 the middle latitudes may explain its occasional, low wintertime data values (e.g., Ploeger et al.,
29 2015a). The trend coefficients are positive for the subtropics of both hemispheres. At this point

1 it is also noted that changes in the BDC based on the CH₄ variations in the southern subtropics
2 can also be affected by the stronger, extratropical wave forcings of the northern hemisphere (see
3 also Sect. 6).

4

5 Estimates of the trends for CH₄ in terms of latitude versus pressure-altitude are shown in Fig. 6.
6 The HALOE CH₄ profiles for this plot are averaged for each of the 12 pressure-altitudes from 0.4
7 hPa to 50 hPa and within 14 overlapping, 20°-wide latitude bins centered from 65°S to 65°N.
8 Trend contours are drawn at intervals of 4 %/decade; the solid contours are positive, while the
9 dashed contours are negative. Positive trends occur at low to middle latitudes and are interpreted
10 as indicating an upward acceleration for the tropical branch of the BDC plus an acceleration
11 poleward. The negative trends or dashed contours at the high latitudes indicate the downward
12 acceleration of the polar branch of the BDC within each hemisphere. Dark shading in Fig. 6 is
13 where the trend term from the MLR model is present with greater than 90% confidence; lighter
14 shading denotes where that confidence is between 70% and 90%. The trend profiles at most
15 latitudes from 50 hPa to about 5 hPa are significant and display a coherent character for an
16 acceleration of an Equator-to-Pole or BDC circulation within each hemisphere, at least during
17 the period of the HALOE measurements. The trends from 50 hPa to about 10 hPa are also
18 clearly asymmetric or positive in the northern hemisphere to near zero in the southern
19 hemisphere. However, the trends in the tropics are of the order of 3 %/decade or equivalent to
20 that expected from the tropospheric source gas (see also Sect. 5).

21

22 **4 Data sampling and data bias concerns**

23 Figure 6 shows that there are rather sharp meridional gradients in the CH₄ trends of the upper
24 stratosphere at 35°N, but not at 35°S. The middle latitudes are where there is often a strong
25 negative meridional gradient in the isolines of CH₄ (c.f., Fig. 2), but the MLR models herein do
26 not have a term to account for a variation with latitude. Rosenlof (2002, her Fig. 4) did not find
27 a similar strong gradient in the trends from her analyses of HALOE profiles, but then she only
28 analyzed data for 1992-2001. A more important difference is that she averaged the HALOE

1 profiles within latitude bins of width 5° , rather than 20° . A narrower bin width is clearly
2 preferred, but there can be a problem with having fewer profiles for the latitude bin. This
3 concern is explored, as follows. First, it is noted that major advantages of solar occultation
4 measurements are the high signal-to-noise for their limb transmission profiles and their
5 inherently good vertical resolution; each retrieved HALOE CH_4 profile is quite accurate and has
6 a vertical resolution of about 4 km (Park et al., 1996). Still, for the lower latitudes HALOE
7 typically made its measurements across a given latitude bin over just a few days, due to the
8 alternating nature of the time sequence of its SR and SS occultations from the UARS satellite.
9 Rosenlof (2002) combined the SR and SS measurements within 5° bins and calculated their
10 monthly averages. However, in the present study the SR and SS profiles are averaged separately.
11 In addition, the exact latitude crossing times for their averages are retained, in order to yield
12 better fits for the AO and especially the SAO terms of the MLR model. Zonal variations for CH_4
13 occur normally at low wavenumber and with small amplitudes compared with its zonal mean
14 value. Thus, a minimum of 5 profiles is required for the separate SR or SS bin averages; that
15 number is judged as representative of the true zonal mean, where the separation between profiles
16 from successive orbits is about 24° longitude. As a check, it was found that requiring a
17 minimum of 7 profiles gave time series having slightly fewer data points, but their analyzed
18 trends were essentially unchanged from before. An exception is at high latitudes during
19 dynamically active winters, but those occurrences are rather short and infrequent across the 14-yr
20 time series of the HALOE measurements.

21

22 To have separate SR and SS samples that are representative of zonal mean CH_4 , a bin width of
23 10° is considered instead for the data points of the time series, and new MLR analyses are carried
24 out. Table 1 compares the resulting trend profiles using bin widths of 10° versus 20° for three
25 selected latitudes of the northern hemisphere. The trend terms that are highly significant are in
26 bold, i.e., having a confidence interval (CI) of being present in the time series that is greater than
27 or equal to 95%. Where the corresponding trends are significant at a given latitude, they are not
28 changed by much using the narrower bins. However, for the upper stratosphere of Table 1 at
29 35°N , the trends are smaller now compared with those found in Fig. 6 using the wider bins.

1 Though not highly significant, those changes are the result of including measured profiles that
2 are more nearly representative of the exact latitude zone of 35°N. The previously large positive
3 trends in the upper stratosphere in Fig. 6 may imply that the location of a given isoline of CH₄
4 moves poleward due to changes in the wave activity and mixing. No similar change is evident
5 for the middle latitudes of the southern hemisphere. An analysis of trends in the transport from
6 an assimilation model is required to really interpret those changes at 35° latitude because the
7 present results from HALOE CH₄ are truly due to the combined effects of the stratospheric age
8 spectra, G, and the loss function, L. The remainder of the paper focuses on trend results obtained
9 from profiles in selected bins of 10° in width.

10

11 Changes in the HALOE instrument have been evaluated in terms of any potential errors for the
12 trends in the data over its 14-yr time series (Gordley et al., 2009). They found that there was a
13 change in the CH₄ gas cell concentration, leading to a false trend in its CH₄ mixing ratio of -
14 1.9 ± 0.7 (1 σ) %/decade that is constant with pressure-altitude. A first order correction for that
15 false trend would be to add 1.9 %/decade to the analyzed trends, although that correction is not
16 applied to the final results herein because it is not obtained strictly through the MLR fit process.
17 A separate concern relates to the pressure profiles associated with the HALOE Level 2 CH₄
18 transmission signals. Specifically, an initial registration for the retrieval uses the temperature
19 versus pressure or T(p) values at 31.5 km altitude from operational data that were supplied to the
20 UARS Project in near real time by the NOAA Climate Prediction Center (CPC) (Thompson and
21 Gordley, 2009). The Level 2 retrieval algorithm for T(p) also uses transmission measurements
22 from the HALOE CO₂ channel that are accurate for the upper stratosphere and mesosphere.
23 There is a weighted merger of the HALOE retrieved T(p) with the CPC profiles over the altitude
24 range of 31.5 to 45 km, such that the final Level 2 T(p) profiles are principally those from the
25 measurements of HALOE down to about the 4-hPa level. Remsberg and Deaver (2005, their
26 Fig. 4) found a discontinuity near May 2001 in the HALOE T(p) times series at 10°N at 5 hPa
27 (near 36 km) but not at 3 hPa, and that shift is traceable to a change in the operational
28 temperatures at that time. However, the retrieved CH₄ mixing ratio versus pressure profiles are

1 in hydrostatic balance. No similar discontinuity is indicated in the time series of the HALOE
2 CH₄ at 10 hPa (Fig. 3), at 7 hPa (Fig. 5), or at the other analyzed levels (not shown).

3

4 **5 Trends in CH₄ from the troposphere and in the stratosphere**

5 It is important to have a good estimate of the trends for the source term, χ_0 , so that its effects can
6 be separated from the product of expression (1), at least to first order. Because there is about a
7 1-yr delay for the surface methane source gas to reach the tropical middle stratosphere, a time
8 frame of 1991-2004 is considered for the time series of the source gas. Methane from remote
9 boundary layer sites was globally-averaged by Dlugokencky et al. (2001; 2009). They showed
10 that the de-seasonalized CH₄ mixing ratios continued to grow during this period, although at
11 rates that were slower from 1992 to 1999 (3.0 %/decade) and from 1999 to 2005 (near zero) than
12 from 1983 to 1992 (4.7 %/decade). Exceptions were the episodic increases at the surface in 1991
13 and 1998 that were followed by equally sharp decreases a year later. An overall trend of 3.0 ± 0.7
14 %/decade is obtained by considering the endpoint values at 1991 and 2004 from their globally-
15 averaged data time series. At the high latitudes the overall trend may be slightly larger because
16 the AoA is older there. Globally-averaged, 1- σ uncertainties from the station data are of the
17 order of 0.6 ppbv/yr, giving the 2- σ value of 0.7 %/decade for the overall trend estimate.

18

19 A separate indication of trends from the CH₄ source term to the stratosphere is obtained for the
20 tropics from the MLR analyses of the HALOE data. Specifically, Fig. 7 shows CH₄ time series
21 at 50 hPa for 5°S and 5°N that are part of the trend results in Fig. 6. Their linear trends and 2 σ
22 uncertainties are 2.8 ± 2.8 and 3.3 ± 3.4 %/decade, respectively, or essentially the same values as
23 from the tropospheric time series, although the tropospheric data have a much smaller
24 uncertainty. The two tropical time series in Fig. 7 have a maximum in late 1992 and a somewhat
25 non-linear (quadratic) character thereafter with a second maximum in 1999. Both maximums
26 follow the observed episodic increases in the troposphere by about a year. The average HALOE
27 trends and 2 σ values are 1.7 ± 2.1 and 3.1 ± 2.1 %/decade at 30 hPa for 5°S and 5°N from Fig. 6;

1 however, the data time series at 30 hPa exhibit very little to no non-linear character (not shown),
2 and that is also the case at the other pressure-altitudes.

3

4 The retrieved HALOE CH₄ mixing ratios in Fig. 7 are only of order 1.4 ppmv in early 1992.
5 Such low values may indicate a slight bias error at 50 hPa, due to a reduced accuracy for the
6 measured and retrieved CH₄ in the presence of the aerosol layer following the eruption of Mt.
7 Pinatubo. However, Thomason (2012) reported that HALOE CH₄ does not appear to be affected
8 by contamination from other minor or trace species within its retrieval algorithm, at least after
9 that early volcanic period. The present study considers data points from mid-1992 and onward
10 for the MLR analyses at all latitudes and pressure-altitudes, primarily to avoid contaminating
11 effects in the lower stratosphere and/or anomalous net transport effects at higher altitudes for
12 some months following the eruption. There is also a small, but clear SR/SS bias in the data of
13 Fig. 7 that is not considered real. Most likely, that bias comes about because of the temperature-
14 pressure-height data from the NOAA CPC that are used to register the HALOE Level 2 mixing
15 ratio profiles in the middle stratosphere. Those provisional data are for 12Z; they do not reflect
16 the effects of the diurnal tide on height and pressure, which are significant in the tropics. No
17 correction is applied to the separate SR and SS time series before they are combined and
18 analyzed, however.

19

20 Time series of CH₄, like those in Figs. 3 and 5, are analyzed at 60°S, 35°S, 10°S, 10°N, 35°N, and
21 60°N, and their latitude bins have a width of 10°. Table 2 contains the mean CH₄ mixing ratio
22 profiles from the constant terms of the MLR models for each of the six latitude zones. The term
23 coefficients show very good symmetry between the two hemispheres in the tropics and at the
24 high latitudes. In the middle to lower stratosphere there is slightly more CH₄ in the southern than
25 in the northern high latitudes, indicating that the net wintertime descent is prolonged and/or a bit
26 stronger in the north. At 50 hPa the mixing ratios are very nearly identical between the two
27 hemispheres for the tropics (1.57 ppmv), middle latitudes (1.34 ppmv), and at high latitudes
28 (1.22 ppmv), indicating that the tropospheric CH₄ that entered the lowest part of the tropical

1 stratosphere is being transported poleward and mixed about equally with the higher latitude air.
2 There is also a monotonic decrease of the CH₄ with altitude in each latitude zone, due to the
3 chemical oxidation of CH₄ to H₂O. The mean CH₄ mixing ratio profiles in Table 2 represent
4 qualitatively the effects of the seasonal BDC transport within each hemisphere.

5

6 The conceptual idea of Plumb (2007, his Figs. 13 and 15) is employed for the detection of an
7 acceleration of the hemispheric BDC using a species like CH₄, whose mixing ratio decreases
8 with altitude as in Figs. 2 and 4. Trends from the HALOE CH₄ time series are interpreted as
9 indicating a change in the strength of the BDC, when they are positive and significantly larger
10 than 3.0 ± 0.7 %/decade in the tropics or significantly smaller or even negative at the high
11 latitudes. Thus, an acceleration of the BDC leads to higher CH₄ values in the tropics and lower
12 values in the extratropics or a steepening of its Equator-to-Pole gradient with time for a given
13 pressure-altitude. On the other hand, the effects of meridional mixing can transport extratropical
14 air back to the subtropics and cause a net recirculation and further aging of the CH₄ (Garny et al.,
15 2014). It is not possible to quantify those separate effects based on the CH₄ observations alone.
16 The analyzed trend terms (%/decade) and the accompanying confidence intervals or CI (in %)
17 for their presence in the time series are given in Table 3. The signs of the trend terms indicate
18 that there is an acceleration of the overall BDC within the middle stratosphere. Note that the
19 highly significant trends are shown by boldface type; they have a CI equal to or greater than 95%
20 of being present in the time series. The trend coefficients are highly significant and different
21 from the trend in χ_o in both the tropics and extratropics from 20 to 7 hPa in the northern
22 hemisphere but only for the tropics from 10 to 5 hPa in the southern hemisphere. It is noted that
23 some of the relatively large trends for the CH₄ time series at high latitudes of the upper
24 stratosphere also carry fairly small uncertainties from the MLR analyses, but those trends are not
25 considered significant because there is non-periodic structure in the time series of their residuals
26 that has not been accounted for.

27

1 Figure 8 is a plot of the trend profiles in %/decade from Table 3 for 10°S and 60°S or within the
2 tropical pipe region of the lower stratosphere and near the edge of the polar vortex region,
3 respectively (Palazzi et al., 2011). Their 2 σ uncertainties are shown as horizontal bars at the
4 tropical levels, where the results are highly significant. Those trends are 17.4 (3.8) at 5 hPa, 13.3
5 (3.6) at 7 hPa, 6.9 (3.1) at 10 hPa, and 1.8 (3.6) at 20 hPa. The vertical dashed line represents the
6 trend of 3.0 (0.7) %/decade, which is the estimate of that for the tropospheric CH₄. The analyzed
7 trend at 5 hPa is large and positive at 10°S and negative at 60°S, so at least their opposing signs
8 are consistent with the expectation for an acceleration of the BDC. The trends at 20 and 10 hPa
9 are positive at both latitudes, although they are less significant at 60°S. On the other hand, there
10 is no evidence for a change of the shallow branch (70 to 30 hPa) of the BDC from these results.
11 The CH₄ trend terms near the stratopause are also insignificant.

12

13 Figure 9 is a plot of the trend profiles from Table 3 at 10°N and 60°N. The highly significant,
14 northern tropical trends and their 2 σ uncertainties are 12.2 (3.4) at 7 hPa, 9.8 (3.2) at 10 hPa,
15 10.0 (3.2) at 20 hPa, 3.8 (4.2) at 30 hPa, and 3.3 (3.0) at 50 hPa. The significant trends for 60°N
16 are -6.3 (20.4) at 5 hPa, -11.3 (14.4) at 7 hPa, -19.5 (9.0) at 10 hPa, and -8.4 (7.6) at 20 hPa.
17 Note that the foregoing trends are still significant after making the first order correction of 1.9
18 %/decade for a change in the HALOE CH₄ gas cell. Trends at 50 hPa and 30 hPa vary from 3.3
19 to 3.8 %/decade at 10°N and from 0.3 to 3.8 %/decade at 60°N, but they carry the same sign and
20 thus disagree with the picture of an acceleration of the hemispheric BDC. Yet, they are
21 consistent with an average trend of 3.0 %/decade for the tropospheric CH₄, indicating that the
22 trends at 60° latitude are merely reflecting a net transport of tropical air to the higher latitudes.
23 The CH₄ trends from 20 hPa to 7 hPa are larger and positive in the tropics, and the corresponding
24 extratropical trends are increasingly negatively up to 10 hPa and remain negative even at 5 hPa.
25 Thus, the signs of the trends from those two northern zones imply that there was an acceleration
26 of the BDC in the middle stratosphere during 1992 to 2005. In other words, an acceleration is
27 indicated for the lower part of the deep branch of the BDC.

28

1 Youn et al. (2006) obtained a positive linear trend at 10 hPa of 9 %/decade at 42.5°S and almost
2 no trend at 42.5°N. For comparison purposes, linear trends are calculated here for 10 hPa and for
3 the same narrow latitude zones of 40 to 45° in each hemisphere. Those trends are 5.7% (6.0) in
4 the southern and -4.6% (10.0) in the northern hemisphere. Possible reasons for the differing
5 results may be that the MLR model of the present study incorporates a larger number of periodic
6 terms plus the effects of autocorrelation among those terms. Coincidentally though, the trends
7 shown in Fig. 6 using the 20°-wide latitude bins are 9.2% (3.0) at 45°S and 0.0% (9.2) at 45°N,
8 which are almost exactly the same values reported by Youn et al. (2006).

9

10 Changes for the BDC in the upper stratosphere are difficult to detect because the photochemical
11 lifetime for the conversion of CH₄ to H₂O is comparable to the time constant for the total
12 transport. The trend in Fig. 8 at 2 hPa is 5.0% (3.2) for 10°S. The trend in Fig. 9 at the same
13 level is smaller and not significant for 10°N or 1.2% (3.9). These findings are at odds with the
14 rather large decreasing trends for CH₄ at the lower latitudes in the upper stratosphere that were
15 reported earlier by Nedoluha et al. (1998, their Fig. 1) for the time span of 1991-1997, by Randel
16 et al. (1999, their Fig. 4) for 1992-1999, and even by Rosenlof (2002) for 1992-2001. An
17 analysis of the HALOE data is carried out for the latitude zone of 10°S to 10°N, but for the entire
18 time period of 1991-2005; the MLR fit to that particular time series is shown in Fig. 10.
19 Qualitatively, the structure in the time series data compares well with that of Nedoluha et al.
20 (1998) from late 1991 through early 1997, and separate analyses conducted here for that early
21 period also give large negative trends. Nevertheless, those trends at 2 hPa did not continue (Fig.
22 10); they are weakly positive or 3.1 %/decade and not significantly different from zero for the
23 complete time series. Coincidentally though, that small trend is consistent with what is estimated
24 from the tropospheric CH₄ source gas data.

25

26 To put the analyzed trends from CH₄ into context for 1992-2005, they are interpreted as follows.
27 First, for the tropics the small positive trends in Figs. 8 and 9 for the lower stratosphere (50 and
28 30 hPa) are equivalent to the average trend of 3.0 %/decade for tropospheric methane; no trend

1 in the BDC is indicated in that region. Note, however, that a correction for the estimated trend in
2 the long-term performance of the HALOE CH₄ gas cell would add about 1.9%/decade to the
3 MLR diagnosed trends herein, or somewhat larger than the average tropospheric trend. A
4 positive trend for CH₄ in this region implies a decreasing (or younger) AoA, which is generally
5 consistent with the AoA estimates of Diallo et al. (2012, Fig. 13) and Monge-Sanz et al. (2012,
6 Fig. 3) from their analyzed winds and heating rates for the period of about 1990-2010. Trends in
7 the tropical HALOE CH₄ mixing ratio are increasing from 30 to 5 hPa and imply that AoA is
8 decreasing in that region, too. In other words, the region where the analyzed CH₄ trends are
9 greater than about 4.9 %/decade corresponds to where AoA estimates ought to be decreasing.
10 This finding differs from the AoA trends of Diallo et al. and Monge-Sanz et al., although it is in
11 reasonable agreement with the findings of Ploeger et al. (2015b, Fig. 2) based on their analyses
12 of AoA trends for 1990-2013. An increase in the CH₄ of the mid to upper tropical stratosphere
13 may have occurred in 1992 due to the effects of the Pinatubo aerosols (Considine et al., 2001;
14 Al-Saadi et al., 2001). That initial acceleration of the BDC was likely followed by an extended
15 period of negative CH₄ trends, as reported by Rosenlof (2002) and Nedoluha et al. (1998).
16 Randel et al. (1999) also reported on a rather episodic rebound for the CH₄ of the lower
17 mesosphere in 1997-1998. However, Fig. 10 indicates that the upward extension of CH₄ at the
18 2-hPa level at that time may have been merely due to interactions with the QBO.

19

20 For the middle latitudes the results in Figure 6 indicate likely contributions from the effects of
21 both horizontal transport and mixing. The trends agree broadly with the early findings of
22 Rosenlof (2002) that were based on HALOE CH₄ from just 1992-2001. Positive CH₄ trends in
23 the middle stratosphere may imply a weakening of the subtropical barriers to transport out of the
24 tropics and toward middle latitudes. This assumption agrees with the decreasing AoA reported
25 by Ploeger et al. (2015b, Fig. 2) for the southern hemisphere. However, it is at odds with their
26 findings for the northern hemisphere, where they found a significant increase in AoA for the
27 period 2002-2012. It is tentatively concluded that there was a decadal change in the CH₄ and the
28 AoA trends and in the BDC for the northern middle latitudes for 1992-2005 versus 2002-2012,
29 related to changes for both the mean meridional circulation and the mixing.

1

2 For the high latitudes Fig. 6 shows negative CH₄ trends at the northern latitudes near 10 hPa that
3 extend equatorward to 50°N, indicating an exchange of vortex air to lower latitudes. No
4 equivalent net equatorward transport is apparent at 10 hPa in the southern hemisphere. Finally,
5 there are hemispheric differences in the CH₄ trends of Fig. 6 for the lower stratosphere, too. In
6 particular, the positive trends at middle latitudes of the northern hemisphere indicate a net
7 poleward transport of younger, tropical air that is consistent with a decrease in the transit time
8 for the shallow branch of the BDC (Bönisch et al., 2011). At southern high latitudes the polar
9 vortex seems to have remained largely intact at higher altitudes. An accelerated descent of the
10 air poleward of 65°S may have extended to below the 20-hPa level, bringing older air to the
11 lower stratosphere where it was mixed efficiently with the air at middle latitudes. Thus, the
12 results in Fig. 6 point to distinct differences in the forcing mechanisms and for the shallow
13 versus the deep branches of the BDC within the two hemispheres.

14

15 **6 Related trends for H₂O and HCl**

16 Supporting evidence is sought from the concurrent trends in HALOE H₂O because CH₄ is
17 oxidized chemically to H₂O in the upper stratosphere; their trends ought to be anti-correlated due
18 to that relationship (Brasseur and Solomon, 2005; Rosenlof, 2002). The mean mixing ratio
19 profiles for H₂O are nearly symmetric for corresponding latitude zones of the two hemispheres
20 (not shown). H₂O values for the subtropics increase from about 3.9 ppmv at 50 hPa to about 6.3
21 ppmv at 0.5 hPa. H₂O also increases slightly from the subtropics to the extratropics in the upper
22 stratosphere, due mostly to the oxidation of CH₄ to H₂O and to its subsequent transport poleward.
23 Seasonal and interannually-varying, entry-level values are found in the HALOE H₂O time series
24 of the tropical lower stratosphere. There is also an episodic decrease in those entry-level values
25 in 2000-2001 (Randel et al., 2006; Fueglistaler, 2012), although that change is nearly
26 imperceptible at 10 hPa in the time series of the middle latitudes. For the lower mesosphere it is
27 presumed that changes are small for the remaining part of the H₂O that is due to the variations of
28 H₂O as it enters the stratosphere through the tropical tropopause, or where the air has an average

1 H₂O mixing ratio of about 3.5 ppmv. Slightly less than half of the H₂O in the lower mesosphere
2 is from the oxidation of methane.

3

4 Trend profiles are obtained from HALOE H₂O using the same terms that were applied in the
5 MLR models for CH₄, and the results are shown and compared for 35°S in Fig. 11 and for 35°N
6 in Fig. 12. In order to get a better idea about their mutual changes, their trend profiles are plotted
7 in terms of ppmv/decade. Estimates of uncertainty are shown by the horizontal bars where the
8 trends are highly significant. The trend terms for H₂O in Fig. 11 are highly significant in the
9 lower stratosphere and also at 0.3 hPa. Trends for H₂O and CH₄ are of the same magnitude and
10 weakly positive in the upper stratosphere, but they are not highly significant. There are
11 indications of an anti-correlation in their mutual trends in Fig. 12 for the upper stratosphere of
12 the northern hemisphere that are more in keeping with that expected from the chemical oxidation
13 of CH₄ to H₂O. Their respective trends also have opposing signs in the lower stratosphere of the
14 northern hemisphere, but that finding is attributed to the trends for those two gases in their
15 tropical source region. In that regard, it is noted that the trend profiles for H₂O in Figs. 11 and
16 12 qualitatively support the modeled trend estimates of stratospheric H₂O for the longer time
17 span of 1986-2010 of Hegglin et al. (2014, their Fig. 5). Their modeled estimates also
18 considered observed trends in tropospheric CH₄ plus a chemical conversion to H₂O.

19

20 Figure 13 is the MLR model fit to the CH₄ time series data at 0.7 hPa of the northern extratropics
21 and subtropics. The minimum in the extratropics occurs in late summer, due to the nearly
22 complete oxidation of the CH₄ at that time. Conversely, there is a maximum in the subtropics in
23 late summer due to the upward diabatic circulation that is a dynamical response to the very warm
24 temperatures of the polar summer stratopause (Andrews et al., 1987). Upon closer inspection,
25 one can readily see that these predominant, annual cycle variations in the data of the extratropics
26 are different for some years; those variations are underestimated by the MLR model terms in
27 1992 and from 2002-2005 and overestimated from 1999-2001. In the subtropics the late summer
28 maximum is overestimated by the model in 1996 and in 2000-2001. The model clearly

1 underestimates the subtropical data in the winter of 1997-98, too. Occasional, seasonal
2 amplitude anomalies are also present in the CH₄ analyses for the southern subtropics but are
3 nearly absent in the southern extratropics (not shown). It is likely that the more pronounced
4 variations in the northern hemisphere are related to the varying planetary wave activity and its
5 effects on the mean meridional transport and mixing of the CH₄. Randel et al. (2000) reported
6 that there was a minimum in the stratospheric wave forcing for the years 1993-1997, followed by
7 an increase in 1998-1999. Pawson and Naujokat (1999) also noted that there were no midwinter
8 warming events for the northern hemisphere in the middle 1990s. Manney et al. (2005) showed
9 that warming events were more prevalent thereafter.

10

11 The seasonal terms of the MLR model simply provide an average fit to the data across all the
12 years. Thus, the time series of HALOE CH₄ of the northern hemisphere indicate that there must
13 be a connection to effects from aperiodic dynamical forcings. For example, the qualitative effect
14 during and just following a warming event is to enhance meridional transport of a tracer (like
15 CH₄) in the upper stratosphere and mesosphere. Hitchman and Leovy (1986) also found that
16 there were secondary residual circulations in the subtropics associated with the descent of the
17 SAO that also responded to stratospheric warming events. The MLR models do not account for
18 the effects of such irregular forcings, and those unmodeled effects can affect the analyzed trends.
19 Thus, it may be that the subtropical trends are merely reflecting the effects of changes in
20 stratospheric wintertime warming activity during 1992-2005, rather than representing any
21 longer-term trend for a change of the deep branch of the BDC at those upper levels. It ought to
22 be possible to verify those instances of MLR/data mismatch with the aid of a model study for a
23 CH₄-like tracer that is transported with the use of assimilated temperature and ozone fields.

24

25 A number of investigators have analyzed time series of HCl in the lower mesosphere to verify
26 concurrent changes in the effects of reactive chlorine on ozone (e.g., Froidevaux et al., 2006).
27 HCl is the primary product of the chemical conversion of free chlorine from methyl chloride and
28 from CFC molecules in the upper stratosphere (Brasseur and Solomon, 2005). For this reason

1 HCl may also be considered as a tracer-like species for studying transport and age-of-air,
2 particularly for the uppermost stratosphere and lower mesosphere. Model studies show peak
3 values of HCl occurring in the lower mesosphere in 1999, while the HCl time series from
4 HALOE at 0.46 hPa and up to 2001 indicate that the observed maximum occurred a year or two
5 earlier or in 1997 (e.g., Waugh et al., 2001). However, the complete time series of HALOE HCl
6 shows two maximums—one in 1997 and another from 2001-2002 (WMO, 2007, Fig. 1-12). It
7 may be that there were significant variations in the observed HCl due to dynamical forcings at
8 those altitudes and that the chemical/transport models do not represent them so well. When the
9 time series of HALOE HCl are referenced to surfaces of constant CH₄, there is better agreement
10 with the modeled trends for HCl in terms of the known changes in its primary surface source
11 gases or the CFCs (James Russell III and John Anderson, Hampton University, private
12 communication, 2002). Thus, it appears that HALOE CH₄ represents a very effective tracer in
13 the lower mesosphere, even though its mixing ratio there is small.

14

15 Spatial gradients for CH₄ and HCl in the lower mesosphere are opposite in sign both vertically
16 and in the meridional direction, such that any anomalies in their respective residuals should have
17 opposing features that would tend to confirm effects from dynamical forcings. Therefore, MLR
18 analyses are applied to time series of both CH₄ and HCl in the lower mesosphere. As shown in
19 Fig. 13, CH₄ has seasonal and QBO-like forcings that are resolved and accounted for reasonably
20 well with the MLR models; the same terms are applied to the HALOE HCl time series. A
21 quadratic term is also added to the linear term for its MLR model because HCl varies non-
22 linearly from 1992-2005. At 55±10°N and 0.7 hPa (near 52 km) the mixing ratio of HCl
23 increases from 2.6 ppbv in 1992 to a maximum of 3.6 ppbv in 2001 and then declines to an
24 average of 3.1 ppbv in 2005; CH₄ at 0.7 hPa is more nearly constant or 0.21 ppmv over that time
25 span.

26

27 Figure 14 (top) shows the time series of the residuals for HCl for 55°N and at 0.7 hPa. The
28 residuals (or data minus MLR model curve values) are obtained in this case by setting the AR-1

1 coefficient to zero, giving a better idea of anomalies for the modeled results. In general, the HCl
2 residuals indicate a good fit to the data, varying between ± 0.2 ppbv or within 6% of the mean for
3 the data. Note though that the residuals are mostly negative in 1998 and 1999 and mostly
4 positive in 1995-1996 and in 2001-2002. Figure 14 (bottom) shows the corresponding residuals
5 for CH₄ that are of the order of ± 0.06 ppmv or about 29% of its mean value; those residuals
6 indicate little to no bias with the model from 1992 to mid-1999, but then show a clear negative
7 bias in 2000 and 2001, or opposite to that from HCl. Thus, there is aperiodic structure remaining
8 in the residuals for both HCl and CH₄, and their opposing signs during some years indicate that a
9 net transport may have been induced by the effects of wave forcings during those winters having
10 significant stratospheric warming activity. Recently though, Damiani et al. (2014) reported that
11 there can also be a chemical re-partitioning of HCl to ClONO₂ in response to a lower
12 mesospheric cooling following stratospheric warming events. The absence of any clear anti-
13 correlation between the HCl and CH₄ residuals of Fig. 14 for 1998-1999 indicates that HCl is not
14 strictly a passive tracer at that time but may be depleted slightly by the chemical repartitioning.
15 That prospect might also explain the small, but anomalous decrease in the HALOE HCl trends of
16 1998-1999 that were reported in WMO (2007).

17

18 **7 Conclusions**

19 Time series data of the tracer-like molecule CH₄ obtained with the UARS HALOE experiment
20 are analyzed using MLR techniques for their periodic and trend terms during 1992-2005. The
21 sunset and sunrise profile data are binned according to tropical and high latitude zones of both
22 the southern and northern hemispheres. The time series are generated and analyzed from 50 hPa
23 to 0.4 hPa. Based on an examination of the data time series, both seasonal and interannual terms
24 are included in the MLR models, in addition to a linear trend term. The trend terms are
25 examined to see whether there is any change in the BDC for the southern or northern
26 hemispheres during 1992-2005 in accordance with the simple concept of Plumb (2007) for a
27 hemispheric BDC. The adoption of that approach indicates that a change of the BDC can be
28 detected where the CH₄ trends are positive by more than 3 %/decade in the tropics and less than
29 that or negative at the high latitudes. Further, since the analyses are conducted at pressure levels

1 rather than at geometric altitudes, it is presumed that any significant trends must be due mainly
2 to changes from the effects of wave forcings on the distributions of CH₄.

3

4 The primary findings of this study are as follows. The CH₄ trend terms for the northern
5 hemisphere are significant and positive from 50 hPa to 7 hPa at 10°N and larger than the
6 tropospheric CH₄ trends of about 3 %/decade from 20 hPa to 7 hPa. At 60°N the trends are
7 clearly negative from 20 hPa to 7 hPa. Thus, the overall trend signature across those two zones
8 indicates an acceleration of the BDC in the middle stratosphere of the northern hemisphere. The
9 CH₄ trends are positive and significant from 10 hPa to 5 hPa for 10°S, and the corresponding
10 trends are negative at 7 hPa and 5 hPa for 60°S but not highly significant; their combined trends
11 do not clearly indicate an acceleration of the BDC for the middle stratosphere of the southern
12 hemisphere. No significant change is indicated for the BDC at 50 and 30 hPa, although the
13 analyzed CH₄ trends are asymmetric between the two hemispheres. The CH₄ trends are also not
14 highly significant for the stratosphere of either hemisphere above the 5-hPa level. The early
15 climate model simulations of Rind et al. (1990) are qualitatively consistent with these findings,
16 in that their model runs show more wave activity and dissipation throughout the winter in the
17 northern than in the southern hemisphere for their model scenario of steady increases of CO₂ in
18 the atmosphere. Still, it may be that these findings of changes in the BDC are only
19 representative of 1992-2005, particularly for the middle latitudes of the northern hemisphere.

20

21 The trends for HALOE H₂O are compared at 35° latitude with those from CH₄ in the upper
22 stratosphere and lower mesosphere because H₂O is the primary product of the oxidation of CH₄
23 at those altitudes. An approximate inverse relationship between their trends is found in the
24 middle and upper stratosphere of the northern hemisphere, but not in the southern hemisphere.
25 The two gases show inverse trends in the lower stratosphere, too. However, while the trends for
26 HALOE H₂O are large and significant in the lower stratosphere, they reflect mostly the episodic
27 decrease for the entry-level H₂O to the stratosphere from below in 2000-2001.

28

1 The variation of CH₄ with time in the lower mesosphere also provides some clues about the
2 effects of aperiodic wave forcings in that region. Other researchers have also reported that there
3 are modest disagreements in the modeled trends for HCl compared to those observed with
4 HALOE, particularly from about 1996 to 2002. Both CH₄ and HCl should serve as tracers of
5 any changes due to the wave forcings. In most instances their respective time series residuals are
6 anti-correlated and support the idea of a dynamical response to wave activity. The observed,
7 small reductions of the HCl in the lower mesosphere for 1998-1999, however, do not seem to be
8 related to a corresponding increase in the CH₄ residuals. A chemical re-partitioning of HCl to
9 ClONO₂ may have occurred at that time. In summary, it is concluded that near-global
10 distributions of CH₄, as remotely measured from a satellite, are an excellent diagnostic of the
11 effects of seasonal and longer-term changes for the total transport within the middle atmosphere.

12

13 *Acknowledgements.* Figure 1 is attributed to Ted Shepherd, Doug Degenstein, and the Optical
14 Spectrograph and InfraRed Imager System (OSIRIS) satellite experiment Team. Figure 2 was
15 kindly provided by Eric Fleming of SSAI and NASA Goddard. The author (EER) appreciates
16 the insightful and helpful comments about his manuscript by the two reviewers. EER carried out
17 this work while serving as a Distinguished Research Associate within the Science Directorate at
18 NASA Langley.

19

1 **References**

2 Al-Saadi, J. A., Pierce, R. B., Fairlie, T. D., Kleb, M. M., Eckman, R. S., Grose, W. L.,
3 Natarajan, M., and Olsen, J. R.: Response of middle atmosphere chemistry and dynamics to
4 volcanically elevated sulfate aerosol: three-dimensional coupled model simulations, *J. Geophys.*
5 *Res.*, 106, D21, 27,255-27,275, 2001.

6

7 Andrews, D. G., Holton, J. R., and Leovy, C. B.: Middle atmosphere dynamics, Academic Press,
8 Inc., Orlando, Florida, 489 pp., 1987.

9

10 Baldwin, M. P., and Dunkerton, T. J.: Biennial, quasi-biennial, and decadal oscillations of
11 potential vorticity in the northern stratosphere, *J. Geophys. Res.*, 103, D4, 3919-3928, 1998.

12

13 Birner, T., and Bönisch, H.: Residual circulation trajectories and transit times into the
14 extratropical lowermost stratosphere, *Atmos. Chem. Phys.*, 11, 817-827, 2011.

15

16 Bönisch, H., Engel, A., Birner, Th., Hoor, P., Tarasick, D. W., and Ray, E. A.: On the structural
17 changes in the Brewer-Dobson circulation after 2000, *Atmos. Chem. Phys.*, 11, 3937-3948,
18 2011.

19

20 Brasseur, G., and Solomon, S.: Aeronomy of the middle atmosphere, 3rd Edition, in *Atmospheric*
21 *and Oceanographic Sciences Library*, vol. 32, Springer, The Netherlands, 644 pp., 2005.

22

23 Butchart, N.: The Brewer-Dobson circulation, *Rev. Geophys.*, 52, 157-184, 2014.

24

1 Considine, D. B., Rosenfield, J. E., and Fleming, E. L.: An interactive model study of the
2 influence of the Mount Pinatubo aerosol on stratospheric methane and water trends, *J. Geophys.*
3 *Res.*, 106, D21, 27,711-27727, 2001.

4

5 Damiani, A., Funke, B., Lopez-Puertas, M., Gardini, A., von Clarmann, T., Santee, M. L.,
6 Froidevaux, L., and Cordero, R. R.: Changes in the composition of the northern polar upper
7 stratosphere in February 2009 after a sudden stratospheric warming, *J. Geophys. Res.*, 119,
8 11,429-11,444, doi:10.1002/2014JD021698, 2014.

9

10 Diallo, M., Legras, B., and Chédin, A.: Age of stratospheric air in the ERA-Interim, *Atmos.*
11 *Chem. Phys.*, 12, 12,133-12,154, doi:10.5194/acp-12-12133-2012, 2012.

12

13 Dlugokencky, E. J., Walter, B. P., Masarie, K. A., Lang, P. M., and Kasischke, E. S.:
14 Measurements of an anomalous global methane increase during 1998, *Geophys. Res. Lett.*, 28,
15 no. 3, 499-502, 2001.

16

17 Dlugokencky, E. J., Bruhwiler, L., White, J. W. C., Emmons, L. K., Novelli, P. C., Montzka, S.
18 A., Masarie, K. A., Lang, P. M., Crotwell, A. M., Miller, J. B., and Gatti, L. V.: Observational
19 constraints on recent increases in the atmospheric CH₄ burden, *Geophys. Res. Lett.*, 36, L18803,
20 doi:10.1029/2009GL039780, 2009.

21

22 Dunkerton, T. J.: On the mean meridional mass motions of the stratosphere and mesosphere, *J.*
23 *Atmos. Sci.*, 35, 2325-2333, 1978.

24

1 Dunkerton, T. J.: Quasi-biennial and subbiennial variations of stratospheric trace constituents
2 derived from HALOE observations, *J. Atmos. Sci.*, 58, 7-25, 2001.

3

4 Fleming, E.L., Jackman, C. H., Stolarski, R. S., and Considine, D. B.: Simulation of stratospheric
5 tracers using an improved empirically based two-dimensional model transport formulation, *J.*
6 *Geophys. Res.*, 104, 23911-23934, 1999.

7

8 Froidevaux, L., Livesey, N. J., Read, W. G., Salawitch, R. J., Waters, J. W., Brouin, B.,
9 MacKenzie, I. A., Pumphrey, H. C., Bernath, P., Boone, C., Nassar, R., Montzka, S., Elkins, J.,
10 Cunnold, D., and Waugh, D.: Temporal decrease in upper atmospheric chlorine, *Geophys. Res.*
11 *Lett.*, 33, L23812, doi:10.1029/2006GL027600, 2006.

12

13 Fueglistaler, S.: Stepwise changes in stratospheric water vapor?, *J. Geophys. Res.*, 117, D13302,
14 doi:10.1029/2012JD017582, 2012.

15

16 Garcia, R. R, Randel, W. J., and Kinnison, D. E.: On the determination of age of air trends from
17 atmospheric trace species, *J. Atmos. Sci.*, 68, 139-154, doi:10.1175/2010JAS3527.1, 2011.

18

19 Garny, H., Birner, T., Boenisch, H., and Bunzel, F.: The effects of mixing on age of air, *J.*
20 *Geophys. Res.*, 119, doi:10.1002/2013JD021417, 2014.

21

22 Gordley, L. L., Thompson, E., McHugh, M., Remsberg, E., Russell III, J., and Magill, B.:
23 Accuracy of atmospheric trends inferred from the halogen occultation experiment, *J. Appl.*
24 *Remote Sensing*, 3, 033526, doi:10.1117/1.3131722, 2009.

1

2 Gray, L. J., and Russell III, J. M.: Interannual variability of trace gases in the subtropical winter
3 stratosphere, *J. Atmos. Sci.*, 56, 977-993, 1999.

4

5 Hall, T. M., and Plumb, R. A.: Age as a diagnostic of stratospheric transport, *J. Geophys. Res.*,
6 99, D1, 1059-1070, 1994.

7

8 Haynes, P. H., Marks, C. J., McIntyre, M. E., Shepherd, T. G., and Shine, K. P.: On the
9 “downward control” of extratropical diabatic circulations by eddy-induced mean zonal forces, *J.*
10 *Atmos. Sci.*, 48, 651-678, 1991.

11

12 Hegglin, M. I., Plummer, D. A., Shepherd, T. G., Scinocca, J. F., Anderson, J., Froidevaux, L.,
13 Funke, B., Hurst, D., Rozanov, A., Urban, J., von Clarmann, T., Walker, K. A., Wang, H. J.,
14 Tegtmeier, S., and Weigel, K.: Vertical structure of stratospheric water vapour trends derived
15 from merged satellite data, *Nature Geoscience*, 7, 768-776, doi:10.1038/ngeo2236, 2014.

16

17 Hitchman, M. H., and Leovy, C. B.: Evolution of the zonal mean state in the equatorial middle
18 atmosphere during October 1978-May 1979, *J. Atmos. Sci.*, 43, 3159-3176, 1986.

19

20 Holton, J. R.: Meridional distribution of stratospheric trace constituents, *J. Atmos. Sci.*, 43, 1238-
21 1242, 1986.

22

23 Holton, J. R., and Choi, W-K.: Transport circulation deduced from SAMS trace species data, *J.*
24 *Atmos. Sci.*, 45, 1929-1939, 1988.

1
2
3
4
5
6
7
8
9
10
11
12
13
14
15
16
17
18
19
20
21
22
23
24

Lin, P., and Fu, Q.: Changes in various branches of the Brewer-Dobson circulation from an ensemble of chemistry climate models, *J. Geophys. Res.*, 118, 73-84, doi:10.1029/2012JD018813, 2013.

Manney, G. L., Zurek, R. W., O'Neill, A., and Swinbank, R.: On the motion of air through the stratospheric polar vortex, *J. Atmos. Sci.*, 51, 2973-2994, 1994.

Manney, G. L., Krüger, K., Sabutis, J. L., Sena, S. A., and Pawson, S.: The remarkable 2003-2004 winter and other recent warm winters in the Arctic stratosphere since the late 1990s, *J. Geophys. Res.*, 110, doi:10.1029/2004JD005367, 2005.

Monge-Sanz, B. M., Chipperfield, M. P., Dee, D. P., Simmons, A. J., and Uppala, S. M.: Improvements in the stratospheric transport achieved by a chemistry transport model with ECMWF (re)analyses: identifying effects and remaining challenges, *Q. J. R. Meteorol. Soc.*, 139, 654-673, 2013.

Nedoluha, G. E., Siskind, D. E., Bacmeister, J. T., Bevilacqua, R. M., and Russell III, J. M.: Changes in upper stratospheric CH₄ and NO₂ as measured by HALOE and implications for changes in transport, *Geophys. Res. Lett.*, 35, 987-990, 1998.

Neu, J. L., Sparling, L. C., and Plumb, R. A.: Variability of the subtropical "edges" in the stratosphere, *J. Geophys. Res.*, 108, D15, 4482, doi:10.1029/2002JD0022706, 2003.

1 Okamoto, K., Sato, K., and Akiyoshi, H.: A study on the formation and trend of the Brewer-
2 Dobson circulation, *J. Geophys. Res.*, 116, D10117, doi:10.1029/2010JD014953, 2011.

3

4 Palazzi, E., Fierli, F., Stiller, G. P., and Urban, J.: Probability density functions of long-lived
5 tracer observations from satellite in the subtropical barrier region: data intercomparison, *Atmos.*
6 *Chem. Phys.*, 11, 10,579-10,598, doi:10.5194/acp-11-10579-2011, 2011.

7

8 Park, J. H., Russell III, J. M., Gordley, L. L., Drayson, S. R., Benner, D. C., McInerney, J. M.,
9 Gunson, M. R., Toon, G. C., Sen, B., Blavier, J-F., Webster, C. R., Zipf, E. C., Erdman, P.,
10 Schmidt, U., and Schiller, C.: Validation of halogen occultation experiment CH₄ measurements
11 from the UARS, *J. Geophys. Res.*, 101, D6, 10,183-10,203, 1996.

12

13 Pawson, S., and Naujokat, B.: The cold winters of the middle 1990s in the northern lower
14 stratosphere, *J. Geophys. Res.*, 104 (D12), 14,209-14,222, 1999.

15

16 Ploeger, F., Riese, M., Haenel, F., Konopka, P., Müller, R., and Stiller, G.: Variability of
17 stratospheric mean age of air and of the local effects of residual circulation and eddy mixing, *J.*
18 *Geophys. Res.*, doi:10.1002/2014JD022468, 2015a.

19

20 Ploeger, F., Abalos, M., Birner, T., Konopka, P., Legras, B., Müller, R., and Riese, M.:
21 Quantifying the effects of mixing and residual circulation on trends of stratospheric mean age of
22 air, *Geophys. Res. Lett.*, doi:10.1002/2014GL062927, 2015b.

23

24 Plumb, R. A.: Tracer interrelationships in the stratosphere, *Rev. Geophys.*, 45, RG4005,
25 doi:10.1029/2005RG000179, 2007.

1
2
3
4
5
6
7
8
9
10
11
12
13
14
15
16
17
18
19
20
21
22
23
24
25

Plumb, R. A., and Ko, M. K. W.: Interrelationships between mixing ratios of long-lived stratospheric constituents, *J. Geophys. Res.*, 97, 10145-10156, 1992.

Randel, W. J., Wu, F., Russell III, J. M., Roche, A., and Waters, J. W.: Seasonal cycles and QBO variations in stratospheric CH₄ and H₂O observed in UARS HALOE data, *J. Atmos. Sci.*, 55, 163-185, 1998.

Randel, W. J., Wu, F., Russell, III, J. M., and Waters, J.: Space-time patterns of trends in stratospheric constituents derived from UARS measurements, *J. Geophys. Res.*, 104, D3, 3711-3727, 1999.

Randel, W. J., Wu, F., Russell III, J. M., Zawodny, J. M., and Nash, J.: Interannual changes in stratospheric constituents and global circulation derived from satellite data, in *Atmospheric Science Across the Stratopause*, (Siskind, D. E.; Eckermann, S. D., and Summers, M. E., Eds.), American Geophysical Union, Washington, D. C., doi:10.1029/GM123p0271, 271-285, 2000,

Randel, W. J., Wu, F., Voemel, H., Nedoluha, G. E., and Forster, P.: Decreases in stratospheric water vapor after 2001: links to changes in the tropical tropopause and the Brewer-Dobson circulation, *J. Geophys. Res.*, 111, D12312, doi:10.1029/2005JD006744, 2006.

Ray, E. A., Moore, F. L, Rosenlof, K. H., Davis, S. M., Sweeney, C., Tans, P., Wang, T., Elkins, J. W., Bönisch, H., Engel, A., Sugawara, S., Nakazawa, T., and Aoki, S.: Improving stratospheric transport trend analysis based on SF₆ and CO₂ measurements, *J. Geophys. Res.*, 119, doi:10.1002/2014JD021802, 2014.

1
2
3
4
5
6
7
8
9
10
11
12
13
14
15
16
17
18
19
20
21
22

Remsberg, E. E.: On the response of Halogen Occultation Experiment (HALOE) stratospheric ozone and temperature to the 11-yr solar cycle forcing, *J. Geophys. Res.*, 113, D22304, doi:10.1029/2008JD010189, 2008.

Remsberg, E. E.: Trends and solar cycle effects in temperature versus altitude from the halogen occultation experiment for the mesosphere and upper stratosphere, *J. Geophys. Res.*, 114, D12303, doi:10.1029/2009JD011897, 2009.

Remsberg, E.: Observed seasonal to decadal scale responses in mesospheric water vapor, *J. Geophys. Res.*, 115, D06306, doi:10.1029/2009JD012904, 2010.

Remsberg, E. E., and Deaver, L. E.: Interannual, solar cycle, and trend terms in middle atmospheric temperature time series from HALOE, *J. Geophys. Res.*, 110, D06106, doi:10.1029/2004JD004905, 2005.

Rind, D., Suozzo, R., Balachandran, N. K., and Prather, M. J.: Climate changes and the middle atmosphere. Part I: the doubled CO₂ climate, *J. Atmos. Sci.*, 47, 475-494, 1990.

Rosenlof, K. H.: Transport changes inferred from HALOE water and methane measurements, *J. Meteorol. Soc. Japan*, 80, 4B, 831-848, 2002.

1 Ruth, S., Kennaugh, R., Gray, L. J., and Russell III, J. M.: Seasonal, semiannual, and interannual
2 variability seen in measurements of methane made by the UARS Halogen Occultation
3 Experiment, *J. Geophys. Res.*, 102, D13, 16189-16199, 1997.

4

5 Scherer, M., Voemel, H., Fueglistaler, S., Oltmans, S. J., and Staehelin, J.: Trends and variability
6 of midlatitude stratospheric water vapour deduced from the re-evaluated Boulder balloon series
7 and HALOE, *Atmos. Chem. Phys.*, 8, 1391–1402, 2008.

8

9 Schoeberl, M. R., Sparling, L. C., Jackman, C. H., and Fleming, E. L.: A Lagrangian view of
10 stratospheric trace gas distributions, *J. Geophys. Res.*, 105, D1, 1537-1552, 2000.

11

12 Shaw, T. A., and Shepherd, T. G.: Raising the roof, *Nature Geoscience*, 1, 12-13, 2008.

13

14 Shepherd, T. G.: Transport in the middle atmosphere, *J. Meteorol. Soc. Japan*, 85B, 165-191,
15 2007.

16

17 Shu, J., Tian, W., Hu, D., Zhang, J., Shang, L., Tian, H., and Xie, F.: Effects of the quasi-
18 biennial oscillation and stratospheric semiannual oscillation on tracer transport in the upper
19 stratosphere, *J. Atmos. Sci.*, 70, doi:10.1175/JAS-D-12-053.1, 2013.

20

21 Solomon, S., Kiehl, J. T., Garcia, R. R., and Grose, W.: Tracer transport by the diabatic
22 circulation deduced from satellite observations, *J. Atmos. Sci.*, 43, 1603-1617, 1986.

23

1 Stanford, J. L., and Ziemke, J. R.: CH₄ and N₂O photochemical lifetimes in the upper
2 stratosphere: in situ estimates using SAMS data, *Geophys. Res. Lett.*, 18, 677-680, 1991.

3

4 Stanford, J. L., Ziemke, J. R., and Gao, S. Y.: Stratospheric circulation features deduced from
5 SAMS constituent data, *J. Atmos. Sci.*, 50, 226-246, 1993.

6

7 Stiller, G. P., von Clarmann, T., Haenel, F., Funke, B., Glatthor, N., Grabowski, U., Kellmann,
8 S., Kiefer, M., Linden, A., Lossow, S., and López-Puertas, M.: Observed temporal evolution of
9 global mean age of stratospheric air for the 2002 to 2010 period, *Atmos. Chem. Phys.*, 12, 3311-
10 3331, doi:10.5194/acp-12-3311-2012, 2012.

11

12 Thomason, L. W.: Toward a combined SAGE II-HALOE aerosol climatology: an evaluation of
13 HALOE version 19 stratospheric aerosol extinction coefficient observations, *Atmos. Chem.*
14 *Phys.*, 12, 8177-8188, 2012.

15

16 Thompson, R. E., and Gordley, L. L.: Retrieval algorithms for the halogen occultation
17 experiment, NASA/CR-2009-215761, available at <http://www.sti.nasa.gov>, 2009.

18

19 Tiao, G. C., Reinsel, G. C., Xu, D., Pedrick, J. H., Zhu, X., Miller, A. J., DeLuisi, J. J., Mateer,
20 C. L., and Wuebbles, D. J.: Effects of autocorrelation and temporal sampling schemes on
21 estimates of trend and spatial correlation, *J. Geophys. Res.*, 95, 20,507-20,517,
22 doi:10.1029/JD095iD12p20507, 1990.

23

1 Volk, C. M., Elkins, J. W., Fahey, D. W., Dutton, G. S., Gilligan, J. M., Loewenstein, M.,
2 Podolske, J. R., Chan, K. R., and Gunson, M. R.: Evaluation of source gas lifetimes from
3 stratospheric observations, *J. Geophys. Res.*, 102, D21, 25,543-25,564, 1997.

4

5 Waugh, D. W., Considine, D. B., and Fleming, E. L.: Is upper stratospheric chlorine decreasing
6 as expected?, *Geophys. Res., Lett.*, 28, 1187-1190, 2001.

7

8 World Meteorological Organization: Scientific assessment of ozone depletion: 2006, Global
9 Ozone Research and Monitoring Project, Report No. 50, Geneva, Switzerland, 2007.

10

11 Youn, D., Choi, W., Lee, H., and Wuebbles, D. J.: Interhemispheric differences in changes of
12 long-lived tracers in the middle stratosphere over the last decade, *Geophys. Res. Lett.*, 33,
13 L03807, doi:10.1029/2005GL024274, 2006.

14

- 1 Table 1. Methane trend profiles (%/decade). Bold denotes trend terms having confidence
 2 intervals (CI) $\geq 95\%$.

P (hPa)	10N	10N	35N	35N	60N	60N
	± 10	± 5	± 10	± 5	± 10	± 5
0.4	10.2	7.7	23.5	12.3	-8.5	-29.6
0.5	9.6	8.7	24.9	8.6	-10.7	-25.2
0.7	3.1	1.5	23.8	4.5	-17.8	-28.0
1.0	-0.6	-4.2	21.3	2.0	-19.0	-22.5
2.0	5.1	1.2	23.4	7.8	-10.3	-3.7
3.0	8.2	8.7	25.4	15.5	-7.2	-3.3
5.0	16.3	20.4	15.7	13.8	-8.3	-6.3
7.0	11.5	12.2	7.7	7.0	-14.2	-11.3
10.0	7.4	9.8	4.2	1.3	-21.3	-19.5
20.0	8.0	10.0	9.7	5.7	-6.7	-8.4
30.0	4.3	3.8	10.7	8.6	0.9	0.3
50.0	3.4	3.3	6.5	6.2	3.4	3.8

3

4

1 Table 2. Mean CH₄ mixing ratio profiles (ppmv).

P (hPa)	60S	35S	10S	10N	35N	60N
0.4	0.20	0.23	0.23	0.24	0.24	0.20
0.5	0.21	0.24	0.25	0.26	0.26	0.20
0.7	0.22	0.28	0.29	0.31	0.30	0.22
1.0	0.23	0.31	0.36	0.40	0.36	0.26
2.0	0.28	0.44	0.57	0.62	0.49	0.35
3.0	0.37	0.56	0.73	0.77	0.56	0.41
5.0	0.53	0.74	0.95	0.96	0.68	0.52
7.0	0.65	0.86	1.11	1.11	0.79	0.63
10.0	0.78	0.98	1.26	1.24	0.90	0.75
20.0	0.98	1.15	1.45	1.42	1.09	0.97
30.0	1.10	1.22	1.52	1.51	1.19	1.06
50.0	1.23	1.35	1.58	1.56	1.34	1.21

2

3

1 Table 3. Southern and northern hemisphere tropical and extratropical CH₄ trend profiles (%
 2 decade⁻¹) and their associated confidence intervals (CI in %) for the presence of the terms in the
 3 MLR models.

4

Pressure (hPa)	60±5°S, CI	10±5°S, CI	10±5°N, CI	60±5°N, CI
0.4	-5.3, 75	8.6, 5	7.7, 34	-29.6, 98
0.5	-7.2, 72	9.4, 7	8.7, 33	-25.2, 93
0.7	-11.0, 83	11.0, 13	1.5, 18	-28.0, 92
1.0	-13.3, 89	5.9, 13	-4.2, 59	-22.5, 78
2.0	-6.2, 60	5.0, 21	1.2, 67	-3.7, 22
3.0	-5.4, 82	15.4, 48	8.7, 11	-3.3, 71
5.0	-3.7, 90	17.4, 97	20.4, 91	-6.3, 99
7.0	-0.7, 57	13.3, 99	12.2, 97	-11.3, 99
10.0	1.0, 7	6.9, 96	9.8, 99	-19.5, 99
20.0	4.0, 69	1.8, 93	10.0, 99	-8.4, 97
30.0	0.1, 7	1.5, 85	3.8, 99	0.3, 2
50.0	-4.1, 62	1.8, 70	3.3, 99	3.8, 84

5

6

7

1 **Figure legends**

2 1. Brewer-Dobson circulation (BDC) and stratospheric ozone. The sense of this net circulation
3 or BDC is shown by the black arrows overlain on the zonally-averaged ozone distribution (or its
4 number density in molecules per cm^3 versus latitude and altitude) for March 2004, as measured
5 by the OSIRIS satellite instrument. Wiggly orange arrow indicates the propagation of waves
6 from the troposphere as they affect the ozone. The dashed black line is the tropopause (adaption
7 of figure in Shaw and Shepherd, 2008).

8

9 2. Methane distribution (ppmv) for January based on a chemistry and transport model
10 simulation. White arrows indicate the sense and strength of the net circulation (image courtesy
11 of Eric Fleming).

12

13 3. Time series of CH_4 is from HALOE at 10 hPa and at 55° latitude for the (top) southern and for
14 the (bottom) northern hemisphere. Solid and open circles indicate the bin-averaged CH_4 data for
15 sunset and sunrise, respectively. The oscillating curve is the MLR fit to the data based on the
16 terms indicated at the lower left, and the near-horizontal line represents the sum of the constant
17 and linear trend terms.

18

19 4. Annually-averaged, zonal mean HALOE methane from the MLR analyses (contour interval is
20 0.2 ppmv).

21

22 5. As in Fig. 3, but at 7 hPa and at 15° latitude for the (top) southern and for the (bottom)
23 northern hemisphere.

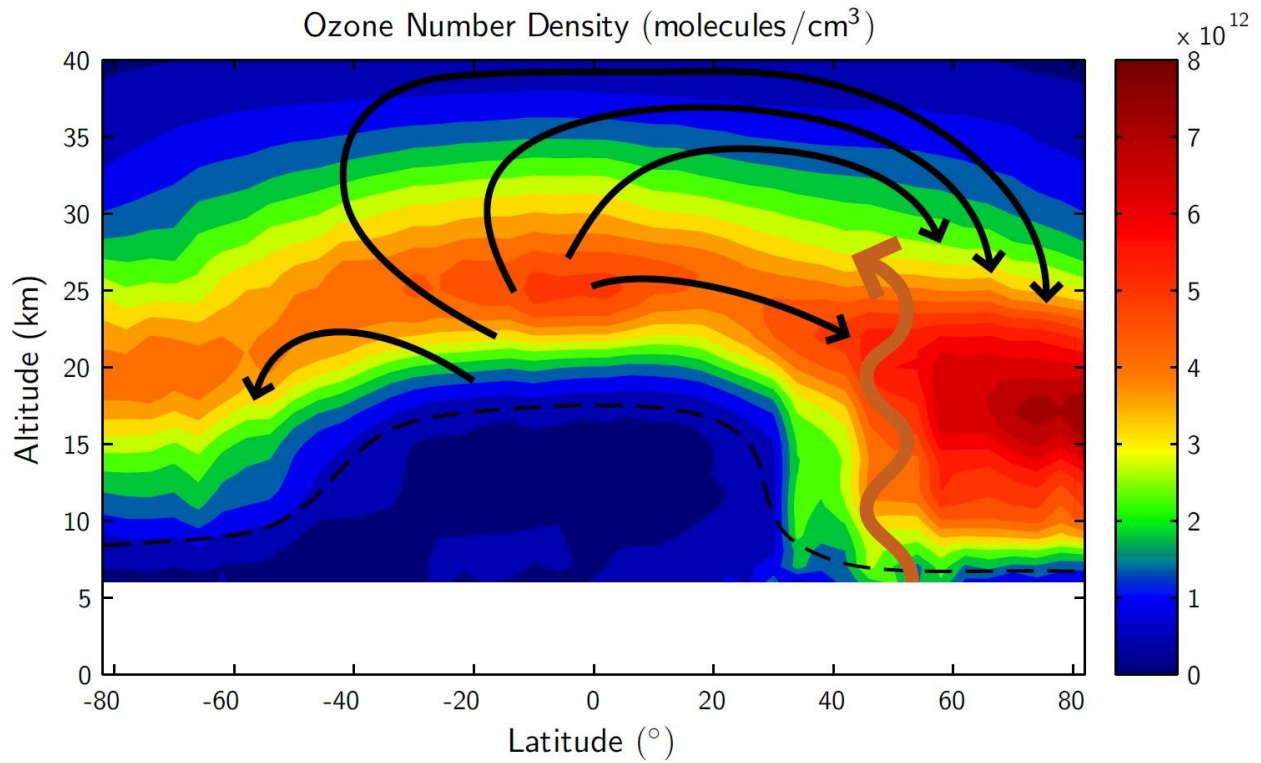
24

- 1 6. Linear trends for HALOE methane (in %/decade). Zero and positive trends are solid contours
2 and negative trends are dashed; contour interval is 4 %/decade. Dark shading denotes where the
3 trends have a confidence interval (CI) $\geq 90\%$, and lighter shading denotes $70\% \leq \text{CI} \leq 90\%$.
- 4
- 5 7. As in Fig. 3, but at 50 hPa and at 5° latitude for the (top) southern and for the (bottom)
6 northern hemisphere.
- 7
- 8 8. Tropical and high latitude trend profiles for CH₄ in the southern hemisphere. Vertical dashed
9 line is the approximate trend for tropospheric CH₄ or 3.0 ± 0.7 %/decade. Horizontal bars show
10 the 2σ error estimates for the highly significant trend terms.
- 11
- 12 9. As in Fig. 8, but for the northern hemisphere.
- 13
- 14 10. Time series of HALOE CH₄ at 2 hPa at the tropical latitudes for comparison with that of
15 Nedoluha et al. (1998).
- 16
- 17 11. Trend profiles (in ppmv/decade) for CH₄ and H₂O at 35° latitude in the southern hemisphere.
18 Horizontal bars denote the 2σ uncertainties for the highly significant trends.
- 19
- 20 12. As in Fig. 11, but for 35° latitude in the northern hemisphere.
- 21
- 22 13. As in Fig. 3, but for CH₄ at 0.7 hPa and at the latitudes of 55° (top) and 15° (bottom) of the
23 northern hemisphere.
- 24

1 14. (top) Time series of HCl residual (data – MLR curve) at 0.7 hPa and at 55°N; (bottom) time
2 series of CH₄ residual at 55°N.

3

4



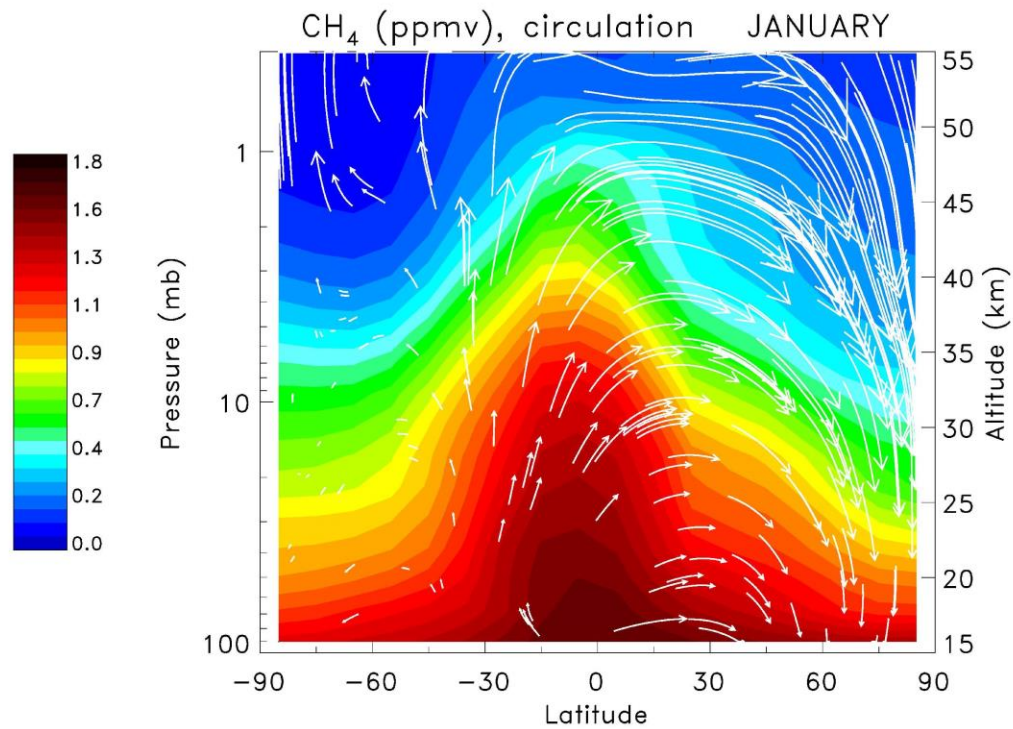
1

2

3 Figure 1. Brewer-Dobson circulation (BDC) and stratospheric ozone. The sense of this net
 4 circulation or BDC is shown by the black arrows overlain on the zonally-averaged ozone
 5 distribution (or its number density in molecules per cm^3 versus latitude and altitude) for March
 6 2004, as measured by the OSIRIS satellite instrument. Wiggly orange arrow indicates the
 7 propagation of waves from the troposphere as they affect the ozone. The dashed black line is the
 8 tropopause (adaption of figure in Shaw and Shepherd, 2008).

9

10

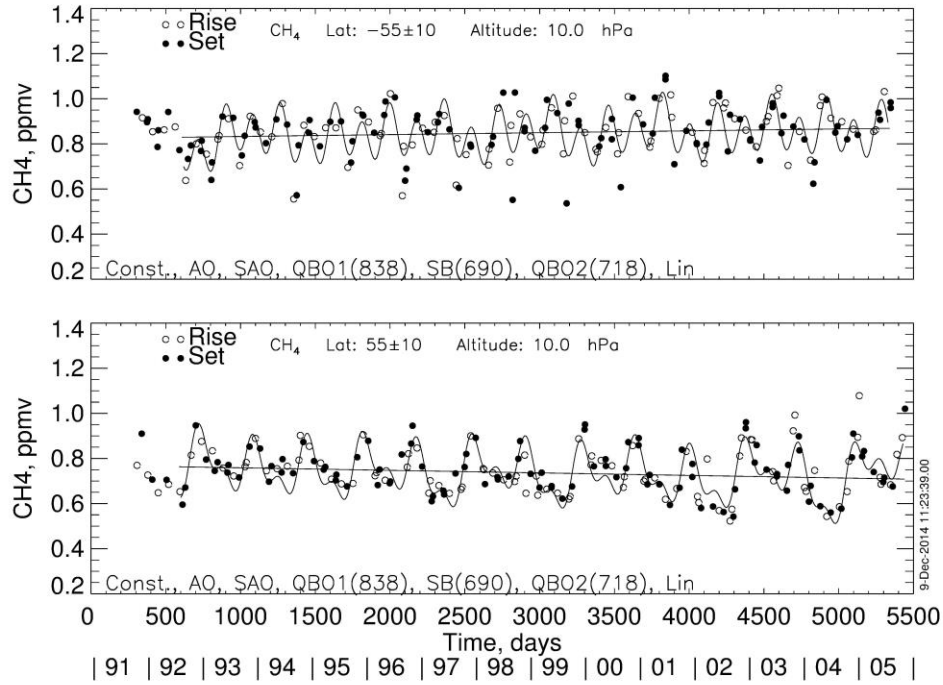


1

2 Figure 2. Methane distribution (ppmv) for January based on a chemistry and transport model
 3 simulation. White arrows indicate the sense and strength of the net circulation (image courtesy
 4 of Eric Fleming).

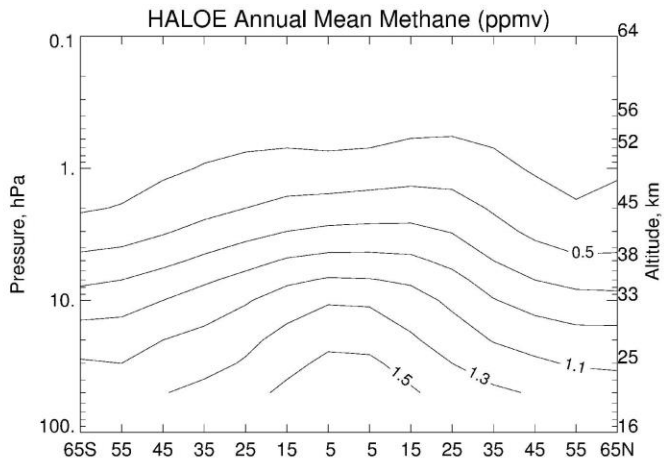
5

6



1
2
3
4
5
6
7
8

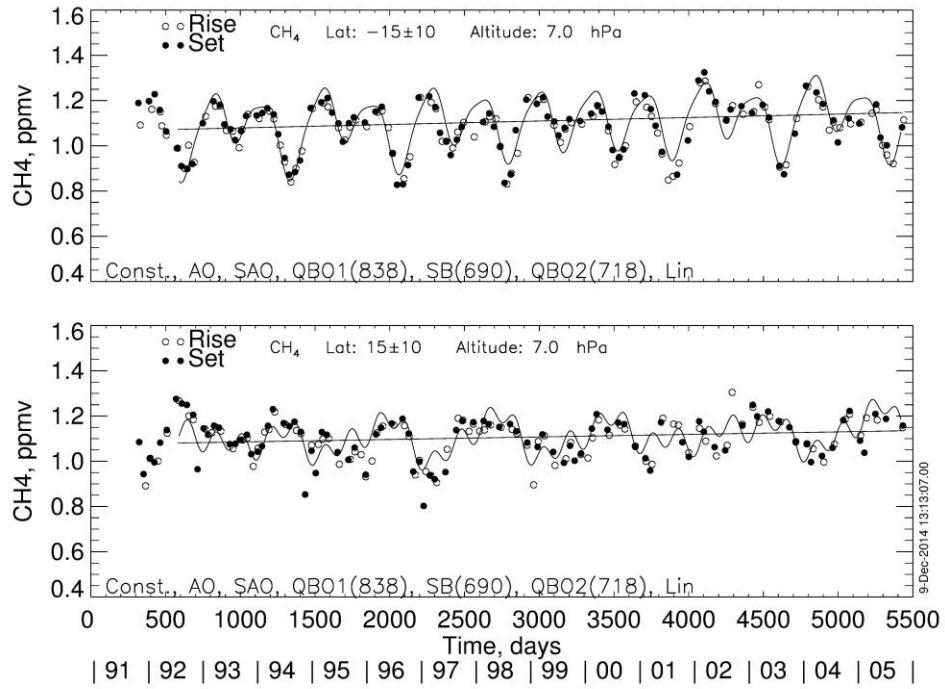
Figure 3. Time series of CH₄ is from HALOE at 10 hPa and at 55° latitude for the (top) southern and for the (bottom) northern hemisphere. Solid and open circles indicate the bin-averaged CH₄ data for sunset and sunrise, respectively. The oscillating curve is the MLR fit to the data based on the terms indicated at the lower left, and the near-horizontal line represents the sum of the constant and linear trend terms.



1

2 Figure 4. Annually-averaged, zonal mean HALOE methane from the MLR analyses (contour
3 interval is 0.2 ppmv).

4



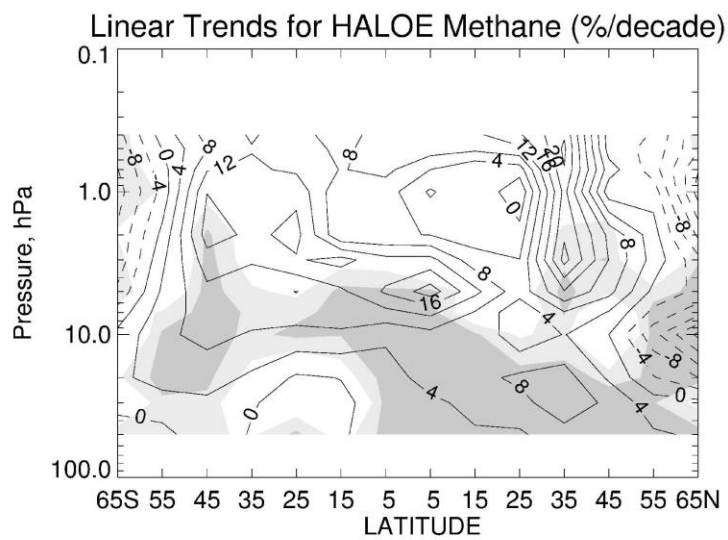
1

2 Figure 5. As in Fig. 3, but at 7 hPa and at 15° latitude for the (top) southern and for the (bottom)

3 northern hemisphere.

4

1

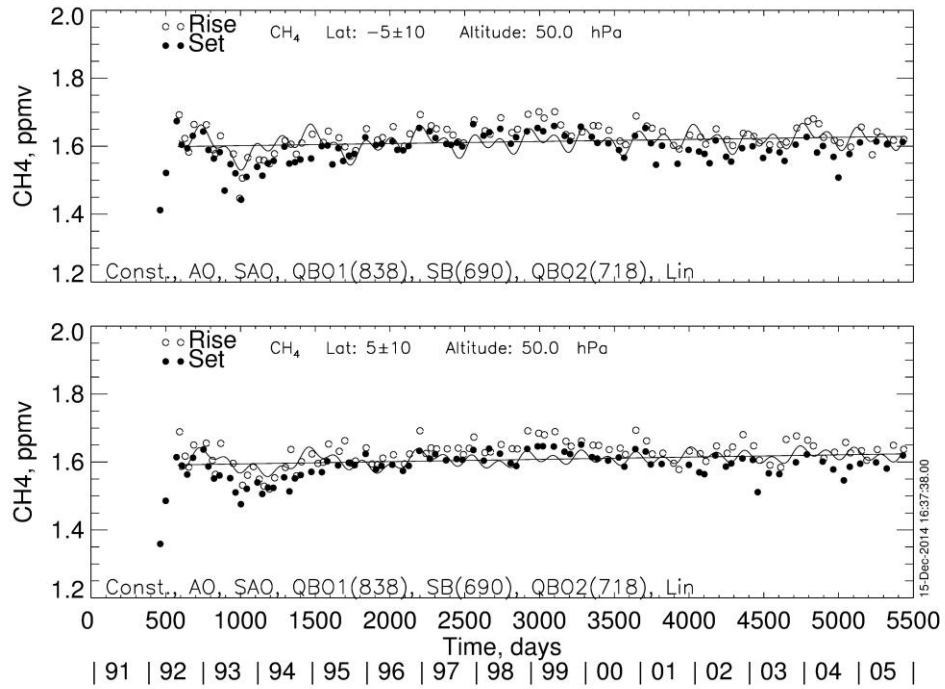


2

3 Figure 6. Linear trends for HALOE methane (in %/decade). Zero and positive trends are solid
4 contours and negative trends are dashed; contour interval is 4 %/decade. Dark shading denotes
5 where the trends have a confidence interval (CI) $\geq 90\%$, and lighter shading denotes $70\% \leq CI <$
6 90% .

7

8



1

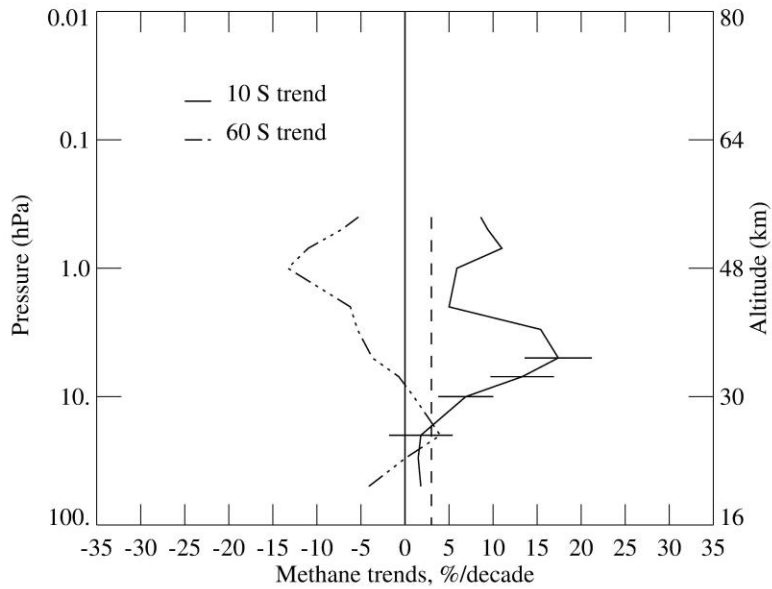
2 Figure 7. As in Fig. 3, but at 50 hPa and at 5° latitude for the (top) southern and for the (bottom)

3 northern hemisphere.

4

5

HALOE Methane Trends, 1992-2005

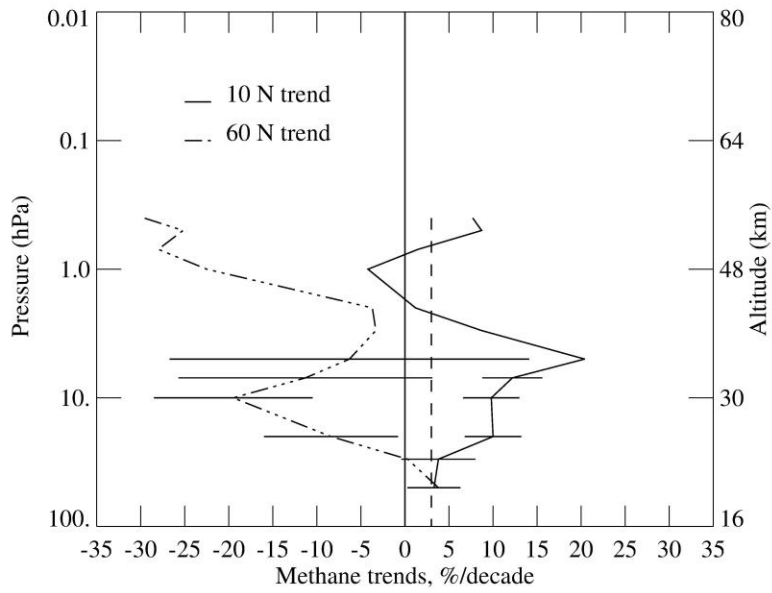


1

2 Figure 8. Tropical and high latitude trend profiles for CH₄ in the southern hemisphere. Vertical
3 dashed line is the approximate trend for tropospheric CH₄ or 3.0±0.7 %/decade. Horizontal bars
4 show the 2σ error estimates for the highly significant trend terms.

5

HALOE Methane Trends, 1992-2005

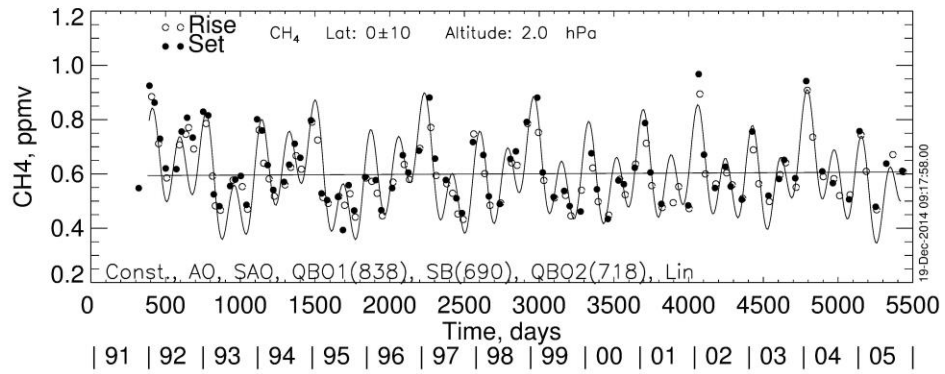


1

2 Figure 9. As in Fig. 8, but for the northern hemisphere.

3

4

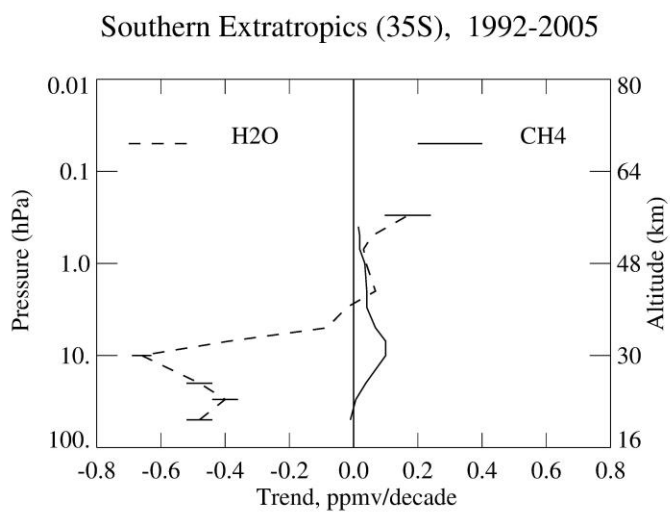


1

2 Figure 10. Time series of HALOE CH₄ at 2 hPa at the tropical latitudes for comparison with that
 3 of Nedoluha et al. (1998).

4

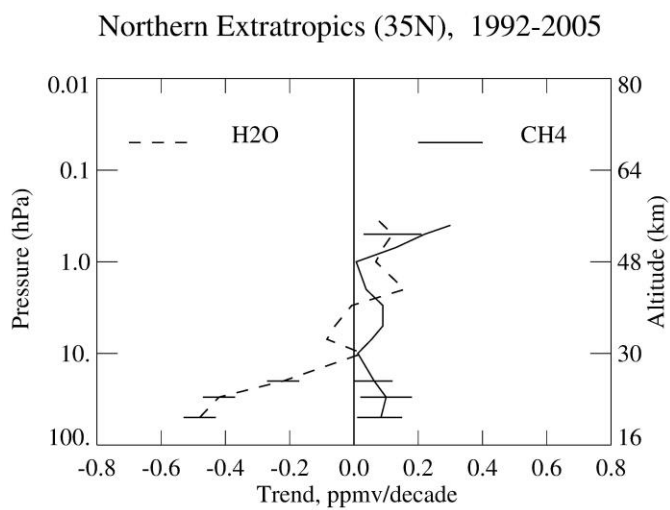
5



1

2 Figure 11. Trend profiles (in ppmv/decade) for CH₄ and H₂O at 35° latitude in the southern
 3 hemisphere. Horizontal bars denote the 2σ uncertainties for the highly significant trends.

4



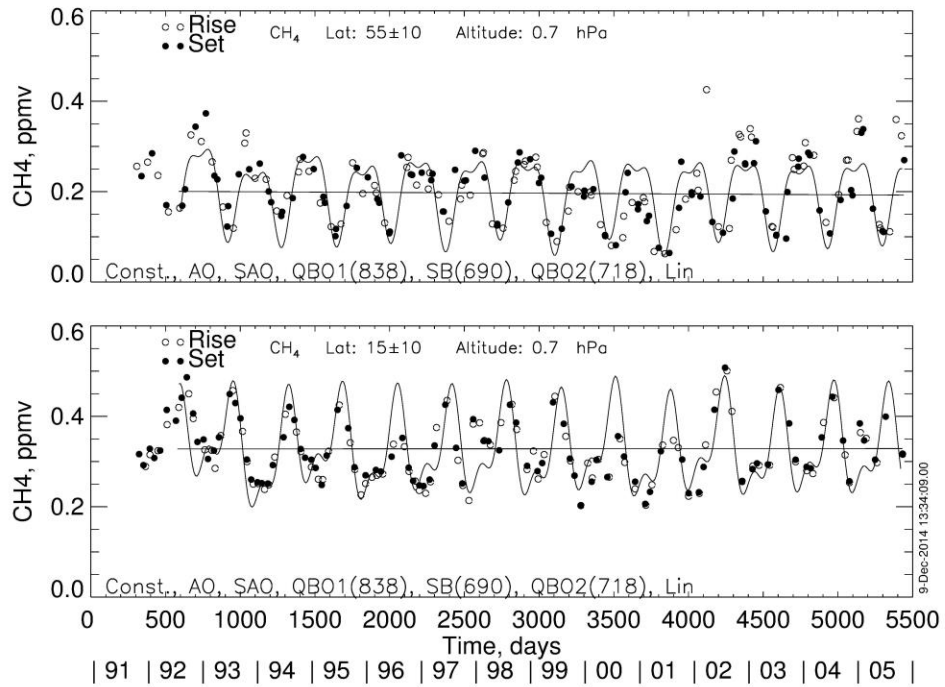
1

2 Figure 12. As in Fig. 11, but for 35° latitude in the northern hemisphere.

3

4

1



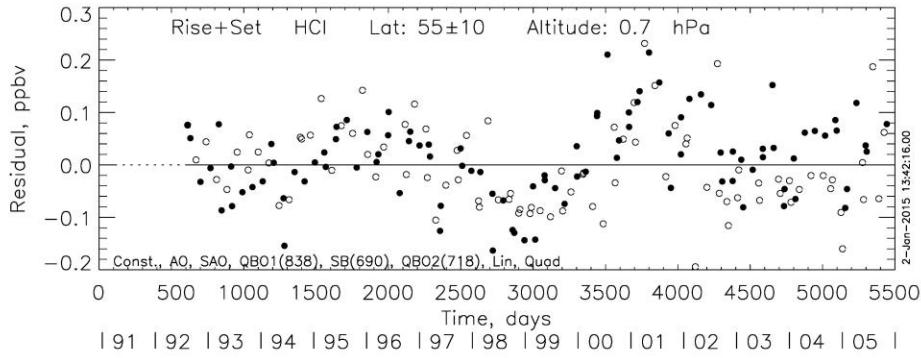
2

3 Figure 13. As in Fig. 3, but for CH₄ at 0.7 hPa and at the latitudes of 55° (top) and 15° (bottom)
4 of the northern hemisphere.

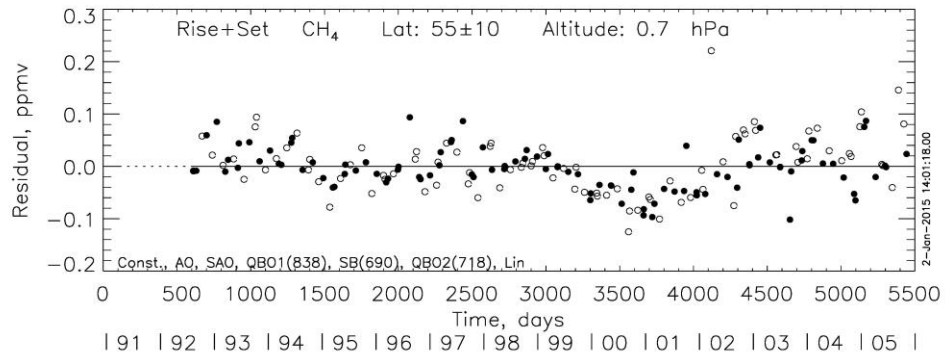
5

6

1



2



3

4 Figure 14. (top) Time series of HCl residual (data – MLR curve) at 0.7 hPa and at 55°N;
5 (bottom) time series of CH₄ residual at 55°N.